INTERNATIONAL CENTER FOR NUMERICAL METHODS IN ENGINEERING

A Rate Dependent Plastic-Damage Constitutive Model for Large Scale Computations in Concrete Structures

R. Faria
X. Oliver

Monografía CIMNE Nº 17, Enero 1993

A Rate Dependent Plastic-Damage Constitutive Model for Large Scale Computations in Concrete Structures

R. Faria
X. Oliver

Monografía Nº 17, Enero 1993

Centro Internacional de Métodos Numéricos en Ingeniería
Gran Capitán s/n, 08034 Barcelona, España

Diseño de la cubierta: Jordi Pallí

Primera Edición, Enero 1993

Edita:
Centro Internacional de Métodos Numéricos en Ingeniería
Edificio C1, Campus Norte UPC
Gran Capitán, s/n
08034 Barcelona, España

ISBN: 84-87867-20 - 0

INDEX

ACKNOWLEDGEMENTS

The authors wish to thank professor J. Lubliner, from the Civil Engineering Department of the University of California at Berkeley, U.S.A., for his valuable contribution to the present work.

The first author wishes to thank the Instituto Nacional de Investigação Científica (Portugal) for a PhD grant, which permitted a valuable stay at the E. T. S. d'Enginyers de Camins, Canals i Ports, Universitat Politècnica de Catalunya, Barcelona, Spain, where the present work was developped.

Chapter 1

INTRODUCTION

1.1 – Structural behavior and safety evaluation of large concrete structures

Since the 1960's, it is possible to assist to the simultaneous development of numerical methods and nonlinear material models. Economical arguments, connected to a greater knowledge demand about structural behavior and its safety evaluation, are some of the reasons by which nonlinear material models tend, nowadays, to be present in almost all fields of civil engineering.

However, such a powerful tool has its own disadvantage. As it is well known, nonlinear material models are essentially large computer-time consumers, which constitutes a serious problem, when dealing with large tridimensional structures.

An example of this scenario is the design of concrete dams, where linear elastic analyses are still today in practice, specially when concerning dynamic computations. Taking into consideration that, for a typical seismic analysis, an accelerogram will contain information abut 1000-2000 time steps, which will require a number of calculations of the same order of magnitude, it is easy to understand why a nonlinear earthquake analysis of, for instance, a tridimensional concrete dam is still today of restricted practical use (Hall (1988)).

Furthermore, many of the nonlinear analyses of dams are performed in order to determine the causes of many observed structural problems (eventually proposing immediate safety remedies), in a *a posteriori* fashion, and only seldom for design purposes.

Koyna Dam (107m high), in India, is probably the most famous example of a concrete dam which experienced serious cracking during an earthquake, which motivated a great number of nonlinear back-analyses, throughout the world-wide scientific community.

More recently, Kölnbrein Arch Dam (200m high), in Austria, was analysed (Linsbauer *et al* (1989a, 1989b)), in order to check for the causes of the extensive cracking observed near the toe of the dam, at the moment the water first attained a level 40m below the maximum. Although in this case the loads responsible for the nonlinear behavior were of static nature (grouting pressure, combined with dead weight and hydrostatic pressure), the complexity of the calculations which were performed called for a simplified analysis, taking into consideration only part of the central cantilever, under plane strain assumption.

This latter example reflects the attention which must be devoted to the kind of nonlinear model to be selected for a large scale computation, in order to capture those features of concrete behavior which should be considered the most relevant for a proper structural nonlinear characterization, but keeping respective computational effort within reasonable limits.

1.2 – Statement of main goals for the election of a concrete material model

In continuation, some particular aspects of constitutive behavior of concrete (specially massive concrete) will be referred, in order to guide towards the election of an appropriate nonlinear material model, physically realistic (for engineering purposes) and computationally fast and easy to implement (in orther to be feasible).

Among the many contributions from experimental analyses of behavior of concrete specimens, it is possible to put in evidence that:

i) Under monotonic uniaxial tests one of the most visible aspects of concrete behavior is that, beyond some stress threshold, it behaves nonlinearly (see figure 1.1), exhibiting progressive and irreversible damage until complete collapse occurs (either in tension or in compression). Bellow the stress threshold, behavior can be considered linear and elastic.

   Under biaxial and triaxial loading similar conclusions can also be taken about concrete behavior, namely the nonlinear branch of the stress-strain curves after an initial threshold.

   This peculiar macroscopic behavior is usually interpreted as a consequence of the fact that concrete is a composite material, with the components:

- a cement matrix, which is a microporous material;

- the aggregates;

- a transition zone between the matrix and the aggregates.

The weakest zone is the last, called halo, because crystals, as a consequence of wall effects, are there highly oriented, leading to a greater porosity (Mazars and Pijaudier-Cabot (1989), Mazars (1991)). Onset of damage occurs in this zone, whenever material strength is lower then the local (microscopic) stress concentration (which enables to understand the existence of a stress threshold, for onset of nonlinearity).

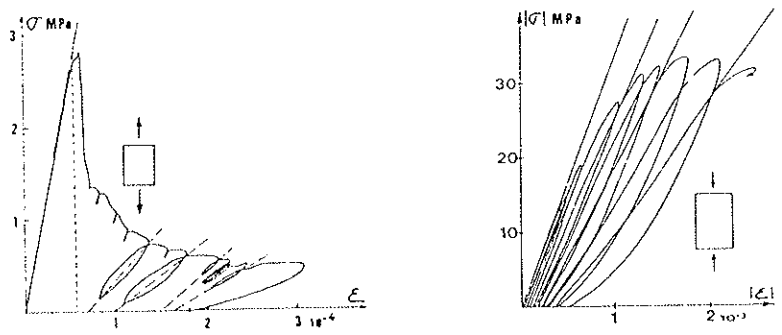

Tension Compression

Figure 1.1 – Uniaxial concrete behavior (Mazars and Pijaudier-Cabot (1989))

Many mechanisms of damage exist, namely the one associated to the propagation of internal microcracks and microvoids (usually inside the cement matrix, following an aleatory and erratic path between the aggregates (Oñate *et al* (1987), or in the cement-aggregate interface (Yankelevsky and Reinhardt (1987)). Another mechanism is the one due to high hydrostatic pressure, leading to consolidation of the material and the collapse of the microporous structure.

ii) Under biaxial and triaxial compressive loading concrete strength is greater that the one observed in uniaxial tests. In biaxial compressive tests it is typical to observe a 1.16-1.20 ratio between biaxial and uniaxial

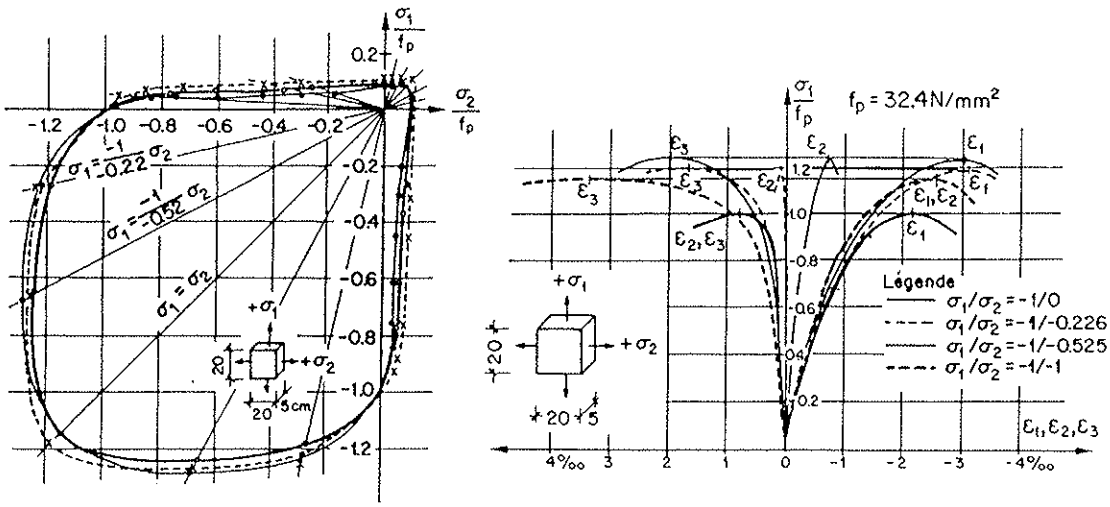

Figure 1.2 – Biaxial concrete behavior (Kupfer *et al* (1969))

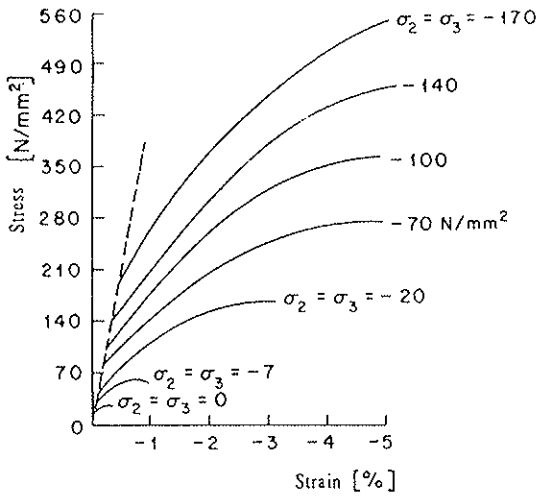

Figure 1.3 – Triaxial concrete behavior (Chen (1982))

strengths (see figure 1.2), but in triaxial tests much greater ratios are reported (see figure 1.3), sometimes attaining values up to 10-20, depending on the confining stresses considered. Although modelling of material behavior under large hydrostatic pressures is obvioulsy out of the scope of the present work, a realistic material model for concrete needs to account for the important feature of strength enhancement under biaxial and triaxial compressive loading.

iii) Beyond the compressive stress threshold, and upon unloading, it is possible to observe that some permanent strains remain (figure 1.1), which is an evidence of the irreversibility inherent to the material loading process. This aspect is an important feature in concrete behavior, and traditionally is referred to as some "plastic strain" (Póvoas (1991), Oñate *et al* (1987)), although some controversy still exists around the pertinence of this concept when applied to geomaterials (CEB (1991), Lubliner *et al* (1989)). These irreversible strains are commonly attributed to the fact that, after occurence of damage, many fissures are distributed among the cement matrix. The roughness of these fissures and the aggregate interlock (CEB (1991)), as well as some slippage, preclude complete closure of cracks, leading to residual strains when concrete is unloaded.

In what concerns earthquake engineering purposes, this plastic effect is an important feature, as it is closely linked to the energy which is dissipated, thus affecting overall structural damping.

iv) When reversing the sign of the external load, it is possible to observe that some stiffness recovering occurs (figure 1.4), when passing from tension to compression (and backwards). This is a macroscopic consequence of the existence of internal microcracks, with capability of selective opening (or closing), depending on the sign of the external load.

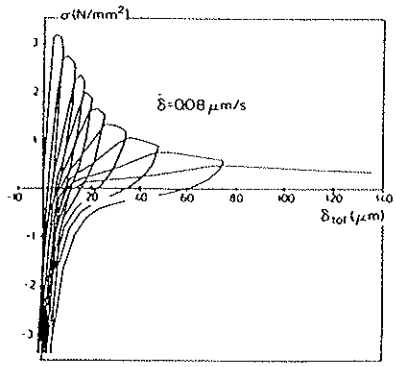

Figure 1.4 – Stiffness recovering (Yankelevsky and Reinhardt (1989))

This phenomenon is also an important feature of concrete behavior, and is termed "unilateral effect" (Mazars and Pijaudier-Cabot (1989), Mazars (1991)). It is obvious that, for dealing with this directional behavior, the nonlinear constitutive law to select for concrete should contain some kind of "memory".

v) When performing experimental uniaxial tests with concrete, but applying loads at increasing speed, it is possible to observe that, when comparing with a quasi-static test, stress-strain curves exhibit decreasing nonlinearity, as well as an increase in both the peak strength and the peak secant modulus (Suaris and Shah (1985), Chappuis (1987)).

It is obvious that microcracking process exhibits rate sensitivity, which is rather more pronounced for tensile than for compressive tests (see figure 1.5).

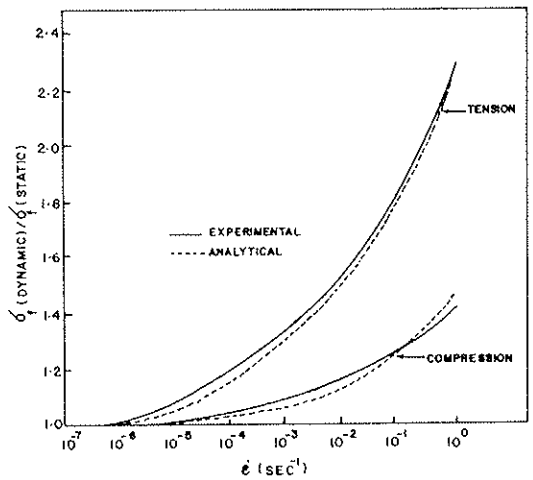

Figure 1.5 – Rate effects on concrete behavior (Suaris and Shah (1984))

If one takes into consideration that under seismic loading deformation rates varying from $10^{-6}/s$ up to $10^{-1}/s$ can be expected (almost the same interval as in figure 1.5) – which is commonly said to be the "impulsive restraint fatigue domain" – it is clear that for earthquake engineering purposes it will be preferable a concrete material model which could accommodate these rate effects.

1.3 – The option for damage models

Having selected the basic features of concrete behavior which must be included in the material model, the next priority is the selection of the nonlinear material model itself.

There is, of course, a wide variety of different material models which could, in principle, satisfy the above requisits (models based on Theory of Hypoelasticity, Hyperelasticity, Plasticity, Fracture Mechanics, Plastic-Fracturing, Endochronic, Microplanes and Damage Mechanics are only some relevant examples (Chappuis (1987), RILEM (1988), Póvoas (1991)).

Keeping in mind that such a model is mainly intended to perform large scale computations, one basic criteria for the selection has to be, of course, the expected computer speed performance, for the same level of information which is obtained.

In the context of the present work, a Damage Model has essentially been selected, with two independent internal damage variables, in order to characterize the (assumed) independent nonlinear mechanisms of degradation of concrete, under tensile or compressive loading conditions. This provides a constitutive law with capability of describing the overall nonlinear stress-strain curves, including the strain-softening response, and the stiffness degradation mechanism (clearly visible in figure 1.1, under multiple loading-unloading conditions). Furthermore, this option has the important advantage of dealing with tensile and compressive concrete behavior in a unified fashion, that is, essentially the same material model is adopted for tension-tension, compression-compression and tension-compression domains (note the algorithmic simplicity which is hence obtained, namely when compared to the rather usual procedure which combines a plasticity derived model for compression-compression domain, a fracture model for tension-tension domain and some arbitrary procedure for tension-compression domains (Póvoas (1991)).

As it will be seen in the next chapters, Damage Mechanics, together with the internal variable concept, provided the general framework in which was possible to develop a very efficient nonlinear material model, with a strain-driven formulation, which lead to an almost closed-form algorithm, where for evaluating the local stress tensor iterations are precluded or rarely needed.

The model which will be described in the next chapters has its own point of departure on the Continuum Damage Mechanics, which is a very powerful and consistent theory, based on the thermodynamics of irreversible processes, firstly introduced by Kachanov (1958) for creep-related problems.

The Continuum Damage Mechanics has a wide range of domains of applicability (creep, fatigue, progressive failure (Chaboche (1988a, 1988b))),

and it is used, nowadays, for materials so different as metal, ceramics, rock and concrete Kachanov (1986)). Such versatility is mainly due to its rigorous thermodynamic foundations, from which not only consistent but also very elegant algorithms are derived.

It was for the aforementioned reasons (rigorous thermodynamic foundations, efficient algorithmic implementation) that a Damage Model has been selected, as the main framework from which a material model for large scale computations of concrete structures has evolved.

By including a plastic strain tensor with a simple but efficient evolution law, the occurrence of irreversible deformations will also be allowed.

Finally, rate dependency will be accounted for as an almost natural extension to the plastic-damage model, introducing a viscous regularization of the evolution laws for the damage variables.

Chapter 2

A MATERIAL DAMAGE MODEL COMBINED WITH PLASTICITY

2.1 – Damage variable concept

For a material being submitted to a particular kind of loading, Continuum Damage Mechanics characterizes its internal damage by means of a set of internal "damage variables", ranging from 0 (virgin undamaged material) to 1 (completely collapsed material) (Lemaitre (1985a)).

In order to clarify the concept of damage, consider a surface element of outwards normal **n** in a damaged material volume. This surface has an area large enough to contain a representative number of defects, but still enabling to be referred as pertaining to a particular material point. If S denotes the overall section area and $\tilde{S}$ the effective resisting area ($S - \tilde{S}$ is the area occupied by the voids), damage variable d associated to direction **n** is, by definition (Lemaitre (1984)):

$$d = \frac{S - \tilde{S}}{S} = 1 - \frac{\tilde{S}}{S} \tag{2.1}$$

As it can be seen, d represents the surface density of material defects, and will have 0 value when material is undamaged, as clearly it will be $S = \tilde{S}$. During the reduction of the effective resisting section area damage will continuously increase, until rupture occurs when some critical value of d is reached (but always $d \leq 1$).

From what it is possible to infer from this definition, damage variable is a non-decreasing quantity, which points out the irreversible characteristic of any material loading process: once some cracking occurs, the effective area is reduced, and no reversibility can exist thereafter. This meaningfull physical reasoning is of capital importance in the context of Continuum (sometimes Continuous) Damage Mechanics, furthermore justifying its denomination.

It must be pointed out that in the above definition damage appears as a directional quantity, which is an important feature for materials exhibiting

highly oriented cracking (Suaris *et al* (1990)), thus leading to important anisotropy. For such materials, tensor-valued damage variables (of rank eight, four or two) (Murakami (1983), Ju (1990)) or at least vector-valued variables (Suaris and Shah (1985)) can be adopted.

In many cases a single scalar representation of damage is adopted, which ensures a sufficiently realistic material model, as it is put in evidence by a great variety of similar models already implemented (Cervera *et al* (1990), Oliver *et al* (1990), Mazars (1991)), furthermore rendering a less complicated algorithm (with reference to tensorial or vectorial alternatives). In this kind of models no particular direction is associated to each damage variable, that is, cracks are assumed to be equally distributed in all directions (Lemaitre (1984)).

2.2 – Effective stress concept

Linked to damage concept, the "effective stress" concept is also a central one in Continuum Damage Mechanics. Although with a very simple definition, its is a meaningfull physical quantity, of capital importance for monitoring material internal processes.

For introducing this concept see figure 2.1, where an overall section area S could be considered (to which the usual Cauchy stress σ is reported), as well $\bar{S}$, which is the effective resisting area (thus, after excluding all the defects).

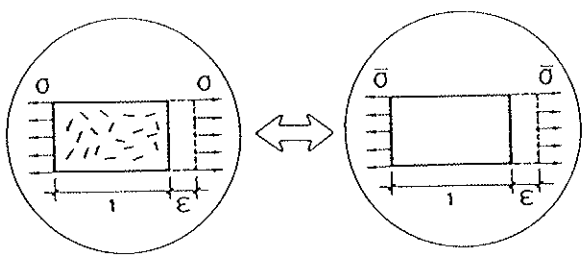

Figura 2.1 – Cauchy stress and effective stress

If one defines the stress $\bar{\sigma}$ such that the following equilibrium equation is

satisfied

$$\sigma\, S = \bar{\sigma}\, \bar{S} \tag{2.2}$$

it is clear that

$$\bar{\sigma} = \sigma \frac{S}{\bar{S}} \tag{2.3}$$

and consequently (by using the damage variable definition),

$$\bar{\sigma} = \frac{\sigma}{1-d} \tag{2.4}$$

which is the definition of the effective stress $\bar{\sigma}$ (Lemaitre (1984)). When a damaging process is occurring, $\bar{\sigma}$ is physically more representative than σ, because in reality it is in the effective stress area that the external loading is resisted, and this is the reason why the powerful effective stress concept has been introduced in Continuum Damage Mechanics. From equation (2.4) it is clear that when damage is null $\bar{\sigma} = \sigma$, and when it approaches 1 the effective stress will tend to infinity.

In connection with the effective stress concept, the *hypothesis of strain equivalence* (Lemaitre and Chaboche (1978)) is also introduced:

> " the strain associated with a damaged state under the applied stress σ is equivalent to the strain associated with its undamaged state under the effective stress $\bar{\sigma}$ " (Simo and Ju (1987a)).

Taking advantage of this hypothesis, together with the already expressed dependency between σ and $\bar{\sigma}$ (equation (2.4)), constitutive laws can be derived in a more comprehensible fashion, by postulating intuitive effective stress-strain relations for material points located on the effective area. For concrete, Cervera *et al* (1991) considered successfully a linear elastic stress-strain assumption in the effective space; in this situation, the nonlinear overall behavior is essentially driven by the effective area reduction, as it is obvious from equation (2.1), thus leading to

$$\sigma = (1-d)\,\bar{\sigma} = (1-d)\,E\,\varepsilon = E'\,\varepsilon$$

in a unidimensional problem (this equation also puts into evidence that damage induces a reduction on the initial elastic Young's modulus, leading to the secant one E').

In the present work the above mentioned strain equivalence will be considered combining elastic and plastic contributions. Considering a general

tridimensional representation, the effective stress tensor $\bar{\boldsymbol{\sigma}}$ (second order) will assume the following form:

$$\boxed{\bar{\boldsymbol{\sigma}} = \mathbf{D_0} : (\boldsymbol{\varepsilon} - \boldsymbol{\varepsilon}^p)} \tag{2.5}$$

In this expression $\mathbf{D_0}$ is the usual fourth order linear-elastic constitutive matrix, $\boldsymbol{\varepsilon}$ is the second order strain tensor, and (:) denotes the tensorial product contracted on two indices. $\boldsymbol{\varepsilon}^p$ is the plastic strain tensor, which reproduces the residual strains visible on concrete upon unloading.

2.3 – Considerations about thermodynamics

Continuum Damage Mechanics is based on the Thermodynamics of the Irreversible Processes (Lemaitre *et al* (1978), Lemaitre (1984), Krajcinovic and Fonseka (1981)), which implies that First and Second Principles of Thermodynamics are systematically obeyed (Lubliner (1972)). This leads to a very consistent framework, in which a non-negative energy dissipation is continuously enforced, according to the irreversible nature of the internal physical processes (this is not always satisfied by other constitutive material models, as it can be seen in Chappuis (1987)).

To establish a particular constitutive law, rigorously founded thermodynamically, a free energy potential must be introduced, where observable and internal variables must be represented (Lubliner (1972)). This potential characterizes the local thermodynamic state, in the sense that distinct equilibrium configurations will have different values for the free energy potential. In this work the strain tensor $\boldsymbol{\varepsilon}$ is selected as the observable variable and $\boldsymbol{\varepsilon}^p$ and the damage variables are the internal ones.

Besides the free energy potential definition, the derivation of a particular constitutive model demands the definition of the kinematics of the internal variables, that is, their evolution laws. In fact a great freedom exists in choosing a particular law (Lemaitre (1984)), providing that a realistic representation of the experimental material behavior is considered, and that a positive (or null) energy dissipation is always obtained (in accordance with the irreversibility of the process).

The free election of the observable and internal variables and of the energy potential which will characterize the material thermodynamic

state, together with the evolution laws, enables to establish a wide variety of thermodynamically consistent material models, with the intended particularities.

In continuation, the relevant steps for developing a plastic-damage model will be presented. For the sake of clarity, rate dependency will be considered in an autonomous chapter, thus avoiding unnecessary complexity of exposure at the present stage.

As a consequence of having selected a scalar damage model, with separeted internal damage variables for tensile and compressive stress contributions, a split of the effective stress tensor into tensile and compressive components will be needed. In order to clearly identify contributions respecting to each one of these independent effective stress tensors, (+) and (−) indices will be extensively used, referring to tensile and compressive entities, respectively. In this work, the stress split will be performed according to

$$\bar{\boldsymbol{\sigma}}^{+} = <\bar{\boldsymbol{\sigma}}> = \sum_{i=1}^{3} <\bar{\sigma}_i> \mathbf{p}_i \otimes \mathbf{p}_i$$

$$\bar{\boldsymbol{\sigma}}^{-} = >\bar{\boldsymbol{\sigma}}< = \sum_{i=1}^{3} >\bar{\sigma}_i< \mathbf{p}_i \otimes \mathbf{p}_i$$

where $\bar{\sigma}_i$ denotes the i-th principal stress from tensor $\bar{\boldsymbol{\sigma}}$ and $\mathbf{p}_i$ represents the unit vector associated to its respective principal direction. The symbols $< . >$ are the MacAuley brackets (thus giving the value of the enclosed expression when positive, and setting a zero value if negative), and symbols $>.<$ are such that $<x>+>x<=x$.

2.4 – Helmholtz free energy potential

Keeping in mind the effective stress tensor introduced by equation (2.5), a possible form for the free energy potential is the Helmholtz free energy. In the present work the following definition (inspired in La Borderie *et al* (1990), Mazars and Pijaudier-Cabot (1989)) will be adopted for this potential:

$$\Psi\left(\boldsymbol{\varepsilon}, \boldsymbol{\varepsilon}^{p}, d^{+}, d^{-}\right) = \left(1-d^{+}\right)\Psi_0^{+}\left(\boldsymbol{\varepsilon}, \boldsymbol{\varepsilon}^{p}\right) + \left(1-d^{-}\right)\Psi_0^{-}\left(\boldsymbol{\varepsilon}, \boldsymbol{\varepsilon}^{p}\right) \tag{2.6}$$

with:

$$\boxed{\Psi_0^+ = \Psi_0^+ (\bar{\boldsymbol{\sigma}}(\boldsymbol{\varepsilon}, \boldsymbol{\varepsilon}^p)) = \frac{1}{2}\, \bar{\boldsymbol{\sigma}}^+ : \mathbf{D_0}^{-1} : \bar{\boldsymbol{\sigma}}} \tag{2.7}$$

$$\boxed{\Psi_0^- = \Psi_0^- (\bar{\boldsymbol{\sigma}}(\boldsymbol{\varepsilon}, \boldsymbol{\varepsilon}^p)) = \frac{1}{2}\, \bar{\boldsymbol{\sigma}}^- : \mathbf{D_0}^{-1} : \bar{\boldsymbol{\sigma}}} \tag{2.8}$$

The entities Ψ_0^+ and Ψ_0^- are elastic free energies and $(1 - d^+)\ \Psi_0^+$ and $(1 - d^-)\ \Psi_0^-$ are the contributions to Ψ, due to the split of $\bar{\boldsymbol{\sigma}}$ effective stress tensor into $\bar{\boldsymbol{\sigma}}^+$ and $\bar{\boldsymbol{\sigma}}^-$ contributions. d^+ and d^- are the damage variables and $\mathbf{D_0}^{-1}$ is the linear-elastic compliance matrix.

Considering the definition of $\mathbf{D_0}^{-1}$

$$\mathbf{D_0}^{-1}_{ijkl} = \mathbf{D_0}^{-1}_{klij} = \frac{1}{E}\Big[(1+\nu)\,\delta_{ik}\,\delta_{jl} - \nu\,\delta_{ij}\,\delta_{kl}\Big] \tag{2.9}$$

and (due to the adopted effective stress split)

$$\bar{\boldsymbol{\sigma}} = \bar{\boldsymbol{\sigma}}^+ + \bar{\boldsymbol{\sigma}}^- \tag{2.10}$$

$$tr\,(\bar{\boldsymbol{\sigma}}) = \bar{\boldsymbol{\sigma}} : \mathbf{I} = tr\,(\bar{\boldsymbol{\sigma}}^+) + tr\,(\bar{\boldsymbol{\sigma}}^-) \tag{2.11}$$

‡ expression (2.7) can be sucessively modified:

$$\begin{aligned}
\Psi_0^+ &= \frac{1}{2}\,\bar{\boldsymbol{\sigma}}^+ : \mathbf{D_0}^{-1} : \bar{\boldsymbol{\sigma}} = \frac{1}{2E}\,\bar{\boldsymbol{\sigma}}^+ : \Big[(1+\nu)\,\bar{\boldsymbol{\sigma}} - \nu\, tr\,(\bar{\boldsymbol{\sigma}})\,\mathbf{I}\Big] = \\
&= \frac{1+\nu}{2E}\,\bar{\boldsymbol{\sigma}}^+ : \bar{\boldsymbol{\sigma}} - \frac{\nu}{2E}\, tr\,(\bar{\boldsymbol{\sigma}})\, tr\,(\bar{\boldsymbol{\sigma}}^+) = \\
&= \frac{1+\nu}{2E}\,\bar{\boldsymbol{\sigma}}^+ : \bar{\boldsymbol{\sigma}} - \frac{\nu}{2E}\, tr^2(\bar{\boldsymbol{\sigma}}^+) - \frac{\nu}{2E}\, tr\,(\bar{\boldsymbol{\sigma}}^-)\, tr\,(\bar{\boldsymbol{\sigma}}^+)
\end{aligned} \tag{2.12}$$

Since

$$\bar{\boldsymbol{\sigma}}^+ : \bar{\boldsymbol{\sigma}}^- = 0 \tag{2.13}$$

---

‡ $tr\,(.)$ is the trace of a tensor.

it is also possible to express Ψ_0^+ according to:

$$\Psi_0^+ = \frac{1+\nu}{2E}\,\bar{\boldsymbol{\sigma}}^+ : \bar{\boldsymbol{\sigma}}^+ - \frac{\nu}{2E}\,tr^2(\bar{\boldsymbol{\sigma}}^+) - \frac{\nu}{2E}\,tr\,(\bar{\boldsymbol{\sigma}}^-)\,tr\,(\bar{\boldsymbol{\sigma}}^+) = \\ = \frac{1}{2}\,\bar{\boldsymbol{\sigma}}^+ : \mathbf{D_0}^{-1} : \bar{\boldsymbol{\sigma}}^+ + \left(-\frac{\nu}{2E}\,tr\,(\bar{\boldsymbol{\sigma}}^-)\,tr\,(\bar{\boldsymbol{\sigma}}^+)\right) \tag{2.14}$$

Owing to its quadratic form, the first additive term of (2.14) is always positive, provided that $\mathbf{D_0}^{-1}$ is a defined and positive matrix. Once $tr\,(\bar{\boldsymbol{\sigma}}^+)$ is positive and $tr\,(\bar{\boldsymbol{\sigma}}^-)$ is negative, the second additive term is also positive, and so

$$\Psi_0^+ \geq 0 \tag{2.15}$$

Using similar reasonings, it is possible to express that

$$\Psi_0^- = \frac{1}{2}\,\bar{\boldsymbol{\sigma}}^- : \mathbf{D_0}^{-1} : \bar{\boldsymbol{\sigma}} = \frac{1}{2}\,\bar{\boldsymbol{\sigma}}^- : \mathbf{D_0}^{-1} : \left(\bar{\boldsymbol{\sigma}}^+ + \bar{\boldsymbol{\sigma}}^-\right) = \\ = \frac{1+\nu}{2E}\,\bar{\boldsymbol{\sigma}}^- : \bar{\boldsymbol{\sigma}}^+ - \frac{\nu}{2E}\,tr\,(\bar{\boldsymbol{\sigma}}^-)\,tr\,(\bar{\boldsymbol{\sigma}}^+) + \frac{1}{2}\,\bar{\boldsymbol{\sigma}}^- : \mathbf{D_0}^{-1} : \bar{\boldsymbol{\sigma}}^- = \\ = \frac{1}{2}\,\bar{\boldsymbol{\sigma}}^- : \mathbf{D_0}^{-1} : \bar{\boldsymbol{\sigma}}^- - \frac{\nu}{2E}\,tr\,(\bar{\boldsymbol{\sigma}}^-)\,tr\,(\bar{\boldsymbol{\sigma}}^+) \geq 0 \tag{2.16}$$

From definition (2.6), and according to equations (2.5, 2.7, 2.8), it is possible to evaluate the expression for the total free energy when no damage and plasticity has yet occurred:

$$\Psi_0 = \Psi_0^+ + \Psi_0^- = \frac{1}{2}\,\bar{\boldsymbol{\sigma}}^+ : \mathbf{D_0}^{-1} : \bar{\boldsymbol{\sigma}} + \frac{1}{2}\,\bar{\boldsymbol{\sigma}}^- : \mathbf{D_0}^{-1} : \bar{\boldsymbol{\sigma}} = \\ = \frac{1}{2}\left(\bar{\boldsymbol{\sigma}}^+ + \bar{\boldsymbol{\sigma}}^-\right) : \mathbf{D_0}^{-1} : \bar{\boldsymbol{\sigma}} = \frac{1}{2}\,\bar{\boldsymbol{\sigma}} : \mathbf{D_0}^{-1} : \bar{\boldsymbol{\sigma}} = \\ = \frac{1}{2}\,\boldsymbol{\varepsilon} : \mathbf{D_0} : \mathbf{D_0}^{-1} : \mathbf{D_0} : \boldsymbol{\varepsilon} = \frac{1}{2}\,\boldsymbol{\varepsilon} : \mathbf{D_0} : \boldsymbol{\varepsilon} \geq 0 \tag{2.17}$$

As it can be observed, Ψ_0 recovers the usual form for the elastic free energy, which is a thermodynamic demand, once for elastic stages the Helmholtz free energy has to equate Ψ_0.

Finally, due to the non-negativeness of Ψ_0^+ and Ψ_0^- and provided that

$$0 \leq d^+ \leq 1 \\ 0 \leq d^- \leq 1 \tag{2.18}$$

it can be concluded that

$$\Psi = (1-d^+)\,\Psi_0^+ + (1-d^-)\,\Psi_0^- \geq 0 \tag{2.19}$$

From the observation of equations (2.6), (2.7) and (2.8) it results that

$$-Y^{+} = -\frac{\partial \Psi}{\partial d^{+}} = \Psi_0^{+} \tag{2.20}$$

$$-Y^{-} = -\frac{\partial \Psi}{\partial d^{-}} = \Psi_0^{-} \tag{2.21}$$

$-Y^{+}$ and $-Y^{-}$ are commonly referred to as being *thermodynamic forces* associated to damage variables d^{+} and d^{-}. Each one of these *forces* is an elastic strain energy release rate associated to a unit damage growth, which gives a physical meaning to the thermodynamic forces, analogous to the Fracture Energy concept in Fracture Mechanics (Lemaitre (1984), Chaboche (1988a)).

2.5 – Characterization of damage

In order to clearly define concepts such as "loading", "unloading", "reloading", a scalar positive quantity, termed *equivalent stress*, will be defined. In essence it is comparable to the dual concept of *equivalent strain* from Simo and Ju (1987a), and enables to compare different tridimensional stress states, evaluating a suitable norm of their respective stress tensors. With such a norm, distinct tridimensional stress states can be mapped to a single *equivalent* unidimensional stress test, which makes possible their quantitative comparison (as it is also common practice in Plasticity (Owen and Hinton (1980))).

As a consequence of the stress split, an equivalent effective tensile stress $\bar{\tau}^{+}$ and an equivalent effective compressive stress $\bar{\tau}^{-}$ will be used. In the present work they will assume the following forms:

$$\bar{\tau}^{+} = \sqrt{\bar{\boldsymbol{\sigma}}^{+} : \mathbf{D}_0{}^{-1} : \bar{\boldsymbol{\sigma}}^{+}} \tag{2.22}$$

$$\bar{\tau}^{-} = \sqrt{\sqrt{3}\,\left(K\,\bar{\sigma}_{oct}^{-} + \bar{\tau}_{oct}^{-}\right)} \tag{2.23}$$

In expression (2.23) K is a material property and $\bar{\sigma}_{oct}^{-}$ and $\bar{\tau}_{oct}^{-}$ are, respectively, the octhaedral normal stress and the octhaedral shear stress[‡], obtained from $\bar{\boldsymbol{\sigma}}^{-}$. Appendix A.1 is devoted to a detailed discussion of equations (2.22) and (2.23), where definition of K is also presented.

With the above definitions for the effective equivalent stresses, two separeted damage criteria g^{+} and g^{-} will be introduced (Simo and Ju (1987a)), the former for tension and the latter for compression:

$$g^{+}(\bar{\tau}^{+}, r^{+}) = \bar{\tau}^{+} - r^{+} \leq 0 \tag{2.24}$$

$$g^{-}(\bar{\tau}^{-}, r^{-}) = \bar{\tau}^{-} - r^{-} \leq 0 \tag{2.25}$$

Variables r^{+} and r^{-} are current damage thresholds, in the sense that their values control the size of the expanding damage surfaces. For the initial stage, that is, when no loading has yet been applied, values r_0^{+} and r_0^{-}, assumed material properties, are attributed to these thresholds.

As it can be deduced from definitions (2.22) and (2.23), equation (2.24) corresponds to a damage bounding surface which is an ellipsoid centered at the origin in the space of principal undamaged tensile stresses (Oliver *et al* (1990)), and equation (2.25) defines a Drucker-Pragger cone for compression (see Appendix A.1 for details).

Equation (2.24) states that tensile damage tends to increase if $\bar{\tau}^{+} = r^{+}$, and so it will be initiated when for the first time $\bar{\tau}^{+} = r_0^{+}$ (a similar reasoning can be applied for compression).

2.6 – Evolution of damage variables

For the evolution of damage variables the following rate equations will be assumed:

- Tension

$$\dot{d}^{+} = \dot{\vartheta}^{+} \frac{\partial G^{+}(\bar{\tau}^{+})}{\partial \bar{\tau}^{+}} \tag{2.26a}$$

$$\dot{\vartheta}^{+} = \dot{r}^{+} \tag{2.26b}$$

---

‡ $\sigma_{oct} = \frac{1}{3} tr\,(\sigma)$;

$\tau_{oct} = \sqrt{\frac{2}{3} J_2}$, where J_2 is the second invariant of the deviatoric stress tensor obtained from σ.

- Compression

$$\dot{d}^- = \dot{\vartheta}^- \frac{\partial G^-(\bar{\tau}^-)}{\partial \bar{\tau}^-} \tag{2.27a}$$

$$\dot{\vartheta}^- = \dot{r}^- \tag{2.27b}$$

with G^+ and G^- being appropriate monotonically increasing functions (derived from experimental observation), in order to accomplish conditions expressed at equation (2.18). $\dot{\vartheta}^+$ and $\dot{\vartheta}^-$ are damage consistency parameters. Using the Kuhn-Tucker relations (Simo and Ju (1987a)), Oliver *et al* (1990)), it is possible to define damage loading or unloading in compacted form (exemplifying for tension):

$$\dot{\vartheta}^+ \geq 0 \qquad g^+ \leq 0 \qquad \dot{\vartheta}^+ g^+ = 0 \tag{2.28}$$

Interpretation of these relations (or of a similar set for compression) is obvious:

. $g^+ < 0$ implies that no further damage is occurring, as it is clearly expressed by last equation in (2.28), which imposes $\dot{\vartheta}^+ = 0$ (equivalent to say, from (2.26a), that no damage evolution exists);

. with $\dot{\vartheta}^+ > 0$ damage is increasing. In this situation $g^+ = 0$, and from the damage consistency condition it will be possible to define $\dot{\vartheta}^+$:

$$g^+(\bar{\tau}^+, r^+) = 0 = const. \quad \Rightarrow \quad \dot{g}^+(\bar{\tau}^+, r^+) = 0 \quad \Rightarrow$$
$$\dot{\bar{\tau}}^+ = \dot{r}^+ = \dot{\vartheta}^+ \tag{2.29}$$

Therefore,

$$r^+ = max\,\{r_0^+,\, max\,(\bar{\tau}^+)\} \tag{2.30}$$

By means of (2.29) and (2.26a) it is possible to define the kinematics of tensile damage variable according to:

$$\dot{d}^+ = \dot{\bar{\tau}}^+ \frac{\partial G^+(\bar{\tau}^+)}{\partial \bar{\tau}^+} = \dot{G}^+ \geq 0 \tag{2.31}$$

For compression it would be obtained:

$$\dot{d}^- = \dot{\bar{\tau}}^- \frac{\partial G^-(\bar{\tau}^-)}{\partial \bar{\tau}^-} = \dot{G}^- \geq 0 \tag{2.32}$$

2.7 – Evolution of plastic strain tensor

As for damage variables, evolution of the plastic strain tensor needs to be introduced, in this work having been considered the following form:

$$\dot{\boldsymbol{\varepsilon}}^p = \beta E H(\dot{d}^-) \frac{\langle \bar{\boldsymbol{\sigma}} : \dot{\boldsymbol{\varepsilon}} \rangle}{\bar{\boldsymbol{\sigma}} : \bar{\boldsymbol{\sigma}}} \mathbf{D}_0^{-1} : \bar{\boldsymbol{\sigma}} \tag{2.33}$$

where E is the Young's modulus and β is supposed to be a material parameter, that controls the rate intensity of plastic deformation (a zero value for this parameter cancels plastic contribution, thus reducing the material model to a elastic-damage one). $H(\dot{d}^-)$ is the Heaviside function of compressive damage rate, and it has been introduced in order to cancel plastic evolution during compressive unloading or partial reloading. The MacAuley brackets enable to set a non-negative value to the product $\bar{\boldsymbol{\sigma}} : \dot{\boldsymbol{\varepsilon}}$, of capital importance for ensuring a non-negative dissipation (section 2.8).

Defining

$$\mathbf{1}_{\bar{\sigma}} = \frac{\bar{\boldsymbol{\sigma}}}{\sqrt{\bar{\boldsymbol{\sigma}} : \bar{\boldsymbol{\sigma}}}} \tag{2.34}$$

equation (2.33) can assume the following contracted form:

$$\dot{\boldsymbol{\varepsilon}}^p = \beta E H(\dot{d}^-) \langle \mathbf{1}_{\bar{\sigma}} : \dot{\boldsymbol{\varepsilon}} \rangle \mathbf{D}_0^{-1} : \mathbf{1}_{\bar{\sigma}} \tag{2.35}$$

The crucial idea underlining the rate equation (2.33) is that plastic strain evolution is assumed to have the direction of the elastic strain tensor $\left(\mathbf{D}_0^{-1} : \bar{\boldsymbol{\sigma}}\right)$, which seems a reasonable assumption (although obviously simplified), in the sense that plasticity is then essentially driven by the effective stress tensor, an entity with physical background.

The link that in the present model has been considered between plasticity and compressive damage evolutions (by means of factor $H(\dot{d}^-)$) was determined by efficiency demands: plastic deformations in reality are present under tensile loading, but have much more relevance under compressive loading. As in fact only an overall effect of plasticity is intended (inducing material damping), the option made seems reasonable. Furthermore, connecting the two mechanisms of nonlinearity – damage and plasticity – avoids evolution of plastic strains during unloading or before the compressive damage threshold is attained (for instance, during the initial elastic branch or during a partial reloading).

2.8 – Dissipation

As stated before, an important feature of Continuum Damage Mechanics is its energetic consistency, which implies that during any loading process dissipation of energy is always a non-negative quantity. This also signifies that entropy will tend to grow, hence leading to an irreversible process, according to the Second Principle of Thermodynamics (Lubliner (1972), Lemaitre (1985b)).

The mathematical expression for this condition is the Clausius-Duhem inequality (Lubliner (1990)), whose reduced form is:

$$\dot{\gamma} = -\dot{\Psi} + \boldsymbol{\sigma} : \dot{\boldsymbol{\varepsilon}} \geq 0 \tag{2.36}$$

where Ψ is the assumed free energy potential and $\boldsymbol{\sigma}$ is the usual Cauchy stress tensor.

In accordance with expression (2.6),

$$\dot{\Psi} = \frac{\partial \Psi}{\partial \boldsymbol{\varepsilon}} : \dot{\boldsymbol{\varepsilon}} + \frac{\partial \Psi}{\partial \boldsymbol{\varepsilon}^p} : \dot{\boldsymbol{\varepsilon}}^p + \frac{\partial \Psi}{\partial d^+} \dot{d}^+ + \frac{\partial \Psi}{\partial d^-} \dot{d}^- \tag{2.37}$$

Substitution into (2.36), also taking into account the derivatives already introduced at equations (2.20, 2.21), it is possible to obtain another expression for the dissipation:

$$\dot{\gamma} = \left(\boldsymbol{\sigma} - \frac{\partial \Psi}{\partial \boldsymbol{\varepsilon}} \right) : \dot{\boldsymbol{\varepsilon}} + \Psi_0^+ \dot{d}^+ + \Psi_0^- \dot{d}^- - \frac{\partial \Psi}{\partial \boldsymbol{\varepsilon}^p} : \dot{\boldsymbol{\varepsilon}}^p \tag{2.38}$$

Due to the fact that $\boldsymbol{\varepsilon}$ is a free variable, an arbitrary $\dot{\boldsymbol{\varepsilon}}$ can be specified. For the equation of dissipation to maintain its generality, the expression within the parenthesis must cancel (Lubliner (1972)). Hence

$$\boldsymbol{\sigma} = \frac{\partial \Psi}{\partial \boldsymbol{\varepsilon}} \tag{2.39}$$

which is one of the Coleman's relations (Lubliner (1972), Simo and Ju (1987a)), essential for the assessment of the constitutive law.

Splitting the current strain tensor $\boldsymbol{\varepsilon}$ into elastic and plastic contributions,

$$\boldsymbol{\varepsilon} = \boldsymbol{\varepsilon}^e + \boldsymbol{\varepsilon}^p \tag{2.40}$$

$$\boldsymbol{\varepsilon}^e = \boldsymbol{\varepsilon} - \boldsymbol{\varepsilon}^p \tag{2.41}$$

the effective stress tensor may be expressed in the form:

$$\bar{\boldsymbol{\sigma}}\left(\boldsymbol{\varepsilon}^{e}\right)=\mathbf{D}_{0}:\left(\boldsymbol{\varepsilon}-\boldsymbol{\varepsilon}^{p}\right)=\mathbf{D}_{0}:\boldsymbol{\varepsilon}^{e} \tag{2.42}$$

and consequently the elastic free energies defined by (2.7, 2.8) are also expressable by:

$$\begin{aligned}\Psi_{0}^{+}\left(\boldsymbol{\varepsilon}^{e}\right)&=\frac{1}{2}\bar{\boldsymbol{\sigma}}^{+}:\mathbf{D}_{0}{}^{-1}:\bar{\boldsymbol{\sigma}}=\frac{1}{2}\bar{\boldsymbol{\sigma}}^{+}:\mathbf{D}_{0}{}^{-1}:\mathbf{D}_{0}:\boldsymbol{\varepsilon}^{e}=\\&=\frac{1}{2}\bar{\boldsymbol{\sigma}}^{+}:\boldsymbol{\varepsilon}^{e}\end{aligned} \tag{2.43}$$

$$\Psi_{0}^{-}\left(\boldsymbol{\varepsilon}^{e}\right)=\frac{1}{2}\bar{\boldsymbol{\sigma}}^{-}:\mathbf{D}_{0}{}^{-1}:\bar{\boldsymbol{\sigma}}=\frac{1}{2}\bar{\boldsymbol{\sigma}}^{-}:\boldsymbol{\varepsilon}^{e} \tag{2.44}$$

The differentiation which is present on equation (2.38) can be decomposed according to the chain rule, thus rendering:

$$\boldsymbol{\sigma}=\frac{\partial\Psi}{\partial\boldsymbol{\varepsilon}}=\frac{\partial\Psi}{\partial\boldsymbol{\varepsilon}^{e}}:\frac{\partial\boldsymbol{\varepsilon}^{e}}{\partial\boldsymbol{\varepsilon}} \tag{2.45}$$

Due to the dependency between $\boldsymbol{\varepsilon}^{e}$ and $\boldsymbol{\varepsilon}$ already expressed at (2.41),

$$\frac{\partial\boldsymbol{\varepsilon}^{e}}{\partial\boldsymbol{\varepsilon}}=\mathbb{I} \tag{2.46}$$

in which $\mathbb{I}$ is the fourth-order identity matrix. So,

$$\boldsymbol{\sigma}=\frac{\partial\Psi}{\partial\boldsymbol{\varepsilon}^{e}}=\left(1-d^{+}\right)\frac{\partial\Psi_{0}^{+}}{\partial\boldsymbol{\varepsilon}^{e}}+\left(1-d^{-}\right)\frac{\partial\Psi_{0}^{-}}{\partial\boldsymbol{\varepsilon}^{e}} \tag{2.47}$$

Once $\bar{\boldsymbol{\sigma}}\left(\boldsymbol{\varepsilon}^{e}\right)$ has a linear dependency on $\boldsymbol{\varepsilon}^{e}$, due to the stress split defined at section 2.3 it is clear that

$$\bar{\boldsymbol{\sigma}}^{+}\left(\alpha\,\boldsymbol{\varepsilon}^{e}\right)=\alpha\,\bar{\boldsymbol{\sigma}}^{+}(\boldsymbol{\varepsilon}^{e}) \tag{2.48}$$

$$\bar{\boldsymbol{\sigma}}^{-}\left(\alpha\,\boldsymbol{\varepsilon}^{e}\right)=\alpha\,\bar{\boldsymbol{\sigma}}^{-}(\boldsymbol{\varepsilon}^{e}) \tag{2.49}$$

(α being some arbitrary scalar). These relations put into evidence that both $\bar{\boldsymbol{\sigma}}^{+}$ and $\bar{\boldsymbol{\sigma}}^{-}$ are homogeneous scalar functions of first degree on $\boldsymbol{\varepsilon}^{e}$, and consequently, according to Euler's theorem[‡]:

$$\bar{\boldsymbol{\sigma}}^{+}(\boldsymbol{\varepsilon}^{e})=\boldsymbol{\varepsilon}^{e}:\frac{\partial\bar{\boldsymbol{\sigma}}^{+}}{\partial\boldsymbol{\varepsilon}^{e}} \tag{2.50}$$

---

‡ Euler's theorem states that if $\varphi(X)$ is a homogeneous function of m-th degree on X, that is,

$$\varphi(\lambda X)=\lambda^{m}\varphi(X)$$

for an arbitrary scalar λ, it occurs that

$$\varphi(X)=\frac{1}{m}X\frac{\partial\varphi}{\partial X}$$

$$\bar{\boldsymbol{\sigma}}^{-}(\boldsymbol{\varepsilon}^{e}) = \boldsymbol{\varepsilon}^{e} : \frac{\partial \bar{\boldsymbol{\sigma}}^{-}}{\partial \boldsymbol{\varepsilon}^{e}} \tag{2.51}$$

In order to clarify the constitutive law (2.47), equation (2.43) must be derived with respect to variable $\boldsymbol{\varepsilon}^{e}$

$$\frac{\partial \Psi_0^{+}}{\partial \boldsymbol{\varepsilon}^{e}} = \frac{1}{2}\frac{\partial \bar{\boldsymbol{\sigma}}^{+}}{\partial \boldsymbol{\varepsilon}^{e}} : \boldsymbol{\varepsilon}^{e} + \frac{1}{2}\bar{\boldsymbol{\sigma}}^{+} \tag{2.52}$$

Calling for equation (2.50), it results that

$$\frac{\partial \Psi_0^{+}}{\partial \boldsymbol{\varepsilon}^{e}} = \frac{1}{2}\bar{\boldsymbol{\sigma}}^{+} + \frac{1}{2}\bar{\boldsymbol{\sigma}}^{+} = \bar{\boldsymbol{\sigma}}^{+} \tag{2.53}$$

Identically, it is easy to conclude that

$$\frac{\partial \Psi_0^{-}}{\partial \boldsymbol{\varepsilon}^{e}} = \bar{\boldsymbol{\sigma}}^{-} \tag{2.54}$$

Hence, the contitutive law defined by (2.47) can be explicited, finally rendering for the Cauchy stress tensor $\boldsymbol{\sigma}$:

$$\boxed{\boldsymbol{\sigma} = (1 - d^{+})\,\bar{\boldsymbol{\sigma}}^{+} + (1 - d^{-})\,\bar{\boldsymbol{\sigma}}^{-}} \tag{2.55}$$

In the equation of dissipation, now reduced to

$$\dot{\gamma} = \Psi_0^{+}\,\dot{d}^{+} + \Psi_0^{-}\,\dot{d}^{-} - \frac{\partial \Psi}{\partial \boldsymbol{\varepsilon}^{p}} : \dot{\boldsymbol{\varepsilon}}^{p} \tag{2.56}$$

the first and second contributions are non-negative quantities, because according to (2.15) and (2.16) Ψ_0^{+}, Ψ_0^{-} are non-negative, and $\dot{d}^{+}$, $\dot{d}^{-}$ are positive (or null), due to the kinematics of damage expressed by (2.31) and (2.32).

So, condition $\dot{\gamma} \geq 0$ will be satisfied once proved the non-negativeness of the last contribution to dissipation. The demonstration will be made keeping in mind that, due to the chain rule,

$$\frac{\partial \Psi}{\partial \boldsymbol{\varepsilon}^{p}} = \frac{\partial \Psi}{\partial \boldsymbol{\varepsilon}^{e}} : \frac{\partial \boldsymbol{\varepsilon}^{e}}{\partial \boldsymbol{\varepsilon}^{p}} \tag{2.57}$$

and that expression (2.33) can be written in compacted form as

$$\dot{\boldsymbol{\varepsilon}}^p = a\,\mathbf{D}_0^{-1} : \bar{\boldsymbol{\sigma}} \tag{2.58}$$

with a being the following non-negative scalar:

$$a = \beta E H(\dot{d}^-)\,\frac{\langle \bar{\boldsymbol{\sigma}} : \dot{\boldsymbol{\varepsilon}} \rangle}{\bar{\boldsymbol{\sigma}} : \bar{\boldsymbol{\sigma}}} \geq 0 \tag{2.59}$$

According to (2.41),

$$\frac{\partial\, \boldsymbol{\varepsilon}^e}{\partial\, \boldsymbol{\varepsilon}^p} = -\mathbb{I} \tag{2.60}$$

and consequently:

$$-\frac{\partial\, \Psi}{\partial\, \boldsymbol{\varepsilon}^p} : \dot{\boldsymbol{\varepsilon}}^p = a\,\frac{\partial\, \Psi}{\partial\, \boldsymbol{\varepsilon}^e} : \mathbf{D}_0^{-1} : \bar{\boldsymbol{\sigma}} \tag{2.61}$$

But equations (2.47) and (2.55) enable to express that

$$\frac{\partial\, \Psi}{\partial\, \boldsymbol{\varepsilon}^e} = \boldsymbol{\sigma} = (1 - d^+)\,\bar{\boldsymbol{\sigma}}^+ + (1 - d^-)\,\bar{\boldsymbol{\sigma}}^- \tag{2.62}$$

which can then be substituted into equation (2.61):

$$-\frac{\partial\, \Psi}{\partial\, \boldsymbol{\varepsilon}^p} : \dot{\boldsymbol{\varepsilon}}^p = a\Big[(1 - d^+)\,\bar{\boldsymbol{\sigma}}^+ : \mathbf{D}_0^{-1} : \bar{\boldsymbol{\sigma}} + (1 - d^-)\,\bar{\boldsymbol{\sigma}}^- : \mathbf{D}_0^{-1} : \bar{\boldsymbol{\sigma}}\Big] \tag{2.63}$$

Insight on the enclosed brackets expression and comparison with definitions (2.6, 2.43, 2.44) puts into evidence that

$$-\frac{\partial\, \Psi}{\partial\, \boldsymbol{\varepsilon}^p} : \dot{\boldsymbol{\varepsilon}}^p = 2\,a\,\Psi \geq 0 \tag{2.64}$$

which is non-negative, once Ψ and a are non-negative quantities‡, thus leading to satisfaction of dissipation inequality:

$$\dot{\gamma} = \Psi_0^+\,\dot{d}^+ + \Psi_0^-\,\dot{d}^- + 2\,a\,\Psi \geq 0 \tag{2.65}$$

---

‡ Now it is clear the reason for having considered the MacAuley brackets in equation (2.33): this way a becomes a positive quantity.

2.9 – Numerical computation of internal variables

For the numerical implementation of the above described model, it will be necessary to specify the procedure for evaluating the damage variables and the plastic strain tensor.

Owing to the fact that the strain tensor $\boldsymbol{\varepsilon}$ is fully determined at the beginning of each step of a displacement-based finite element algorithm, a strain-based scheme for updating d^+, d^- and $\boldsymbol{\varepsilon}^p$ will be presented, rendering an almost closed-form algorithm (with obvious computational efficiency).

2.9.1 – Damage variables

The particular forms assumed by the rate equations (2.31) and (2.32) allow to specify the following damage evolution laws, after performing a trivial integration (with the initial condition of null damages):

$$d^+ = G^+(\bar{\tau}^+) \tag{2.66}$$

$$d^- = G^-(\bar{\tau}^-) \tag{2.67}$$

These equations put into evidence that, once specified the strain tensor, damage variables can be easily evaluated, as they only depend on the equivalent stresses $\bar{\tau}^+$ and $\bar{\tau}^-$, which are evaluated from $\boldsymbol{\varepsilon}$.

So, the selection for the particular forms of functions G^+ and G^- will determine the specific damage evolutions to be considered, and consequently some care must be devoted to this subject, so that a realistic representation of experimental behavior might be obtained. Anyway, the change from one particular set of evolution laws to a different one does not put any special problem, thus enabling this model to have substantial updating versatility.

For the present work, the following damage evolution rules will be adopted:

- Tension

$$d^+ = 1 - \frac{r_0^+}{\bar{\tau}^+}\, e^{A^+\left(1-\frac{\bar{\tau}^+}{r_0^+}\right)} \tag{2.68}$$

• Compression

$$d^- = 1 - \frac{r_0^-}{\bar{\tau}^-}(1 - A^-) - A^- e^{B^-(1-\frac{\bar{\tau}^-}{r_0^-})} \tag{2.69}$$

both capable to ensure that

$$0 \leq d^+ \leq 1$$
$$0 \leq d^- \leq 1$$

Equation (2.68) is able to reproduce the softening branch of a concrete unidimensional tensile test, asymptotically to the strain axis, as it is an observational evidence (Lubliner *et al* (1989)). With this evolution law for d^+, due to Oliver *et al* (1990), a finite area is retained between the stress-strain curve and the strain axis, which is crucial to appropriately define the fracture energy concept (as it is well known, of primary importance to satisfy requisits of mesh-objectivity when dealing with softening materials, as it happens for concrete under tensile loading (Bažant *et al* (1979a), Bažant *et al* (1983)). Besides the tensile damage threshold r_0^+ (usually corresponding to the uniaxial tensile peak strength), only the parameter A^+ exists, the determination of which is made by equating the material fracture energy to the time integral of dissipation (see Appendix A.2 for details). Oliver *et al* (1990) obtained excellent results with this evolution law, in the context of an isotropic model with a single damage variable.

By means of equation (2.69) it is possible to reproduce the hardening effect on concrete submitted to compression, as well the softening wich occurs after the compressive strength is attained (Mazars and Pijaudier-Cabot (1989)). In figure 2.3 it is demonstrated that with this evolution law a fairly good representation of concrete experimental behavior is obtained. Besides r_0^-, for its characterization two parameters (A^-, B^-) must be defined, usually by imposing that the evolution curve satisfies two selected points of a unidimensional experimental test (see Appendix A.2 for details).

2.9.2 – Plastic strain tensor

The particular evolution law proposed on equation (2.33) has the important advantage of enabling to define a fast numerical algorithm for updating the effective plastic stress tensor, as it will be proved in this section.

Performing differentiation with respect to time of equation (2.5) and taking (2.33) into consideration, the following expression can be obtained:

$$\dot{\bar{\boldsymbol{\sigma}}} = \mathbf{D_0} : (\dot{\boldsymbol{\varepsilon}} - \dot{\boldsymbol{\varepsilon}}^p) = \mathbf{D_0} : \dot{\boldsymbol{\varepsilon}} - \beta EH(\dot{d}^-) \langle \bar{\boldsymbol{\sigma}} : \dot{\boldsymbol{\varepsilon}} \rangle \frac{\bar{\boldsymbol{\sigma}}}{\bar{\boldsymbol{\sigma}} : \bar{\boldsymbol{\sigma}}} \tag{2.70}$$

Introducing a backward-Euler difference scheme, denoting by $(.)_{t+\Delta t}$ entities respecting to the actual time-step and by $(.)_t$ the entities already determined in the previous time-step, and using the standard $\Delta(.)$ notation for incremental entities, the numerical integration procedure will be:

$$\bar{\boldsymbol{\sigma}}_{t+\Delta t} = \bar{\boldsymbol{\sigma}}_t + \mathbf{D_0} : \Delta\boldsymbol{\varepsilon} - \beta EH(\dot{d}^-_{t+\Delta t}) \langle \bar{\boldsymbol{\sigma}}_{t+\Delta t} : \Delta\boldsymbol{\varepsilon} \rangle \frac{\bar{\boldsymbol{\sigma}}_{t+\Delta t}}{\bar{\boldsymbol{\sigma}}_{t+\Delta t} : \bar{\boldsymbol{\sigma}}_{t+\Delta t}} \tag{2.71}$$

where further simplification could be introduced by setting

$$\bar{\boldsymbol{\sigma}}^T = \bar{\boldsymbol{\sigma}}_t + \mathbf{D_0} : \Delta\boldsymbol{\varepsilon} \tag{2.72}$$

and

$$\| \bar{\boldsymbol{\sigma}} \| = \sqrt{\bar{\boldsymbol{\sigma}} : \bar{\boldsymbol{\sigma}}} \tag{2.73}$$

thus rendering (performing some mathematics):

$$\left\{ \frac{\| \bar{\boldsymbol{\sigma}}_{t+\Delta t} \|^2 + \beta EH(\dot{d}^-_{t+\Delta t}) \langle \bar{\boldsymbol{\sigma}}_{t+\Delta t} : \Delta\boldsymbol{\varepsilon} \rangle}{\| \bar{\boldsymbol{\sigma}}_{t+\Delta t} \|} \right\} \frac{\bar{\boldsymbol{\sigma}}_{t+\Delta t}}{\| \bar{\boldsymbol{\sigma}}_{t+\Delta t} \|} = \bar{\boldsymbol{\sigma}}^T \tag{2.74}$$

Considering definition (2.34) for $\mathbf{1}_{\bar{\boldsymbol{\sigma}}_{t+\Delta t}}$, and the next one for θ,

$$\theta = \| \bar{\boldsymbol{\sigma}}_{t+\Delta t} \| + \beta EH(\dot{d}^-_{t+\Delta t}) \langle \mathbf{1}_{\bar{\boldsymbol{\sigma}}_{t+\Delta t}} : \Delta\boldsymbol{\varepsilon} \rangle \tag{2.75}$$

it results

$$\theta \, \mathbf{1}_{\bar{\boldsymbol{\sigma}}_{t+\Delta t}} = \bar{\boldsymbol{\sigma}}^T \tag{2.76}$$

from which it is evident that (evaluating the norms of both members):

$$\theta = \| \bar{\boldsymbol{\sigma}}^T \| \tag{2.77}$$

This conclusion can be used to define equation (2.76) in an alternative way, that is:

$$\theta \, \mathbf{1}_{\bar{\boldsymbol{\sigma}}_{t+\Delta t}} = \| \bar{\boldsymbol{\sigma}}^T \| \, \mathbf{1}_{\bar{\boldsymbol{\sigma}}^T} = \theta \, \mathbf{1}_{\bar{\boldsymbol{\sigma}}^T} \tag{2.78}$$

where use of equation (2.34) was made once more, for defining $\mathbf{1}_{\bar{\boldsymbol{\sigma}}^T}$. Direct observation of equation (2.78) puts into evidence that

$$\mathbf{1}_{\bar{\boldsymbol{\sigma}}_{t+\Delta t}} = \mathbf{1}_{\bar{\boldsymbol{\sigma}}^T} \tag{2.79}$$

and so equation (2.75) can assume the form

$$\| \bar{\boldsymbol{\sigma}}^T \| = \| \bar{\boldsymbol{\sigma}}_{t+\Delta t} \| + \beta E H(\dot{d}^-_{t+\Delta t}) \langle \mathbf{1}_{\bar{\boldsymbol{\sigma}}^T} : \Delta\boldsymbol{\varepsilon} \rangle \tag{2.80}$$

or alternatively

$$\| \bar{\boldsymbol{\sigma}}_{t+\Delta t} \| = \| \bar{\boldsymbol{\sigma}}^T \| - \beta E H(\dot{d}^-_{t+\Delta t}) \langle \mathbf{1}_{\bar{\boldsymbol{\sigma}}^T} : \Delta\boldsymbol{\varepsilon} \rangle \tag{2.81}$$

Hence, the effective stress tensor can be evaluated according to

$$\begin{aligned} \bar{\boldsymbol{\sigma}}_{t+\Delta t} &= \| \bar{\boldsymbol{\sigma}}_{t+\Delta t} \| \, \mathbf{1}_{\bar{\boldsymbol{\sigma}}_{t+\Delta t}} = \| \bar{\boldsymbol{\sigma}}_{t+\Delta t} \| \, \mathbf{1}_{\bar{\boldsymbol{\sigma}}^T} = \\ &= \left(\| \bar{\boldsymbol{\sigma}}^T \| - \beta E H(\dot{d}^-_{t+\Delta t}) \langle \mathbf{1}_{\bar{\boldsymbol{\sigma}}^T} : \Delta\boldsymbol{\varepsilon} \rangle \right) \mathbf{1}_{\bar{\boldsymbol{\sigma}}^T} = \\ &= \left(1 - \frac{\beta}{\| \bar{\boldsymbol{\sigma}}^T \|} E H(\dot{d}^-_{t+\Delta t}) \langle \mathbf{1}_{\bar{\boldsymbol{\sigma}}^T} : \Delta\boldsymbol{\varepsilon} \rangle \right) \bar{\boldsymbol{\sigma}}^T \end{aligned} \tag{2.82}$$

from which it is clear that, once known $H(\dot{d}^-_{t+\Delta t})$, evaluation of $\bar{\boldsymbol{\sigma}}_{t+\Delta t}$ can be performed directly, as $\Delta\boldsymbol{\varepsilon}$, $\bar{\boldsymbol{\sigma}}^T$ and $\mathbf{1}_{\bar{\boldsymbol{\sigma}}^T}$ are fully explicit quantities, due to their strain-driven characteristics. The form of equation (2.82) puts into evidence that the updating of $\bar{\boldsymbol{\sigma}}_{t+\Delta t}$ is inspired in a *radial return algorithm*: $\bar{\boldsymbol{\sigma}}^T$ can be looked as a predictor tensor, from which the effective stress tensor can be obtained once evaluated the scale factor α:

$$\alpha = 1 - \frac{\beta}{\| \bar{\boldsymbol{\sigma}}^T \|} E H(\dot{d}^-_{t+\Delta t}) \langle \mathbf{1}_{\bar{\boldsymbol{\sigma}}^T} : \Delta\boldsymbol{\varepsilon} \rangle \tag{2.83}$$

Numerical procedure for computing the effective stress tensor is then only reduced to the evaluation of α. Note that $\alpha \leq 1$, which means that

$$\| \bar{\boldsymbol{\sigma}}_{t+\Delta t} \| \leq \| \bar{\boldsymbol{\sigma}}^T \| \tag{2.84}$$

As only a single doubt exists in equation (2.82) (the 0 or 1 value for the Heaviside function), determination of the new effective stress tensor can be performed in a double-trial procedure. Box 2.1 presents the algorithm implemented within the context of the present work for determining the effective stress tensor, when plasticity is intended. It is instructive to see that as

$$\bar{\boldsymbol{\sigma}}_{t+\Delta t} = \alpha \, \bar{\boldsymbol{\sigma}}^T \quad ,$$

according to (2.84), and denoting by $\left(\bar{\tau}^T\right)^-$ the equivalent stress associated to the negative split of $\bar{\boldsymbol{\sigma}}^T$ tensor, the following inequality applies:

$$\bar{\tau}^-_{t+\Delta t} \leq \left(\bar{\tau}^T\right)^- \tag{2.85}$$

which means that if $\left(\bar{\tau}^T\right)^- < r^-_t$ obviously $\bar{\tau}^-_{t+\Delta t} < r^-_t$ and $\dot{d}^-_{t+\Delta t} = 0$, and so no plastic evolution occurs (a quick exit from the algorithm devoted to the evaluation of compressive damage and plasticity can then be performed).

Box 2.1 – Evaluation of elasto-plastic effective stress tensor

INPUT: β, E, $\mathbf{D}_0$, $\bar{\boldsymbol{\sigma}}_t$, $\triangle\boldsymbol{\varepsilon}$, r_t^-

OUTPUT: $\bar{\boldsymbol{\sigma}}_{t+\triangle t}$

ALGORITHM:

(1) Evaluate $\bar{\boldsymbol{\sigma}}^T = \bar{\boldsymbol{\sigma}}_t + \mathbf{D}_0 : \triangle\boldsymbol{\varepsilon}$

(2) Split into $\left(\bar{\boldsymbol{\sigma}}^T\right)^+$ and $\left(\bar{\boldsymbol{\sigma}}^T\right)^-$ and calculate $\left(\bar{\tau}^T\right)^-$, according to (2.23). Check for $\left(\bar{\tau}^T\right)^- > r_t^-$?

YES: Proceed to step (3).

NO: No compressive damage and no plastic evolution exist. Set $\bar{\boldsymbol{\sigma}}_{t+\triangle t} = \bar{\boldsymbol{\sigma}}^T$. EXIT.

(3) Evaluate $\mathbf{1}_{\bar{\boldsymbol{\sigma}}^T}$, according to (2.34), and $\| \bar{\boldsymbol{\sigma}}^T \|$.

(4) Check for $\langle \mathbf{1}_{\bar{\boldsymbol{\sigma}}^T} : \triangle\boldsymbol{\varepsilon} \rangle > 0$?

YES: Plasticity is possible. Compute

$$\alpha = 1 - \frac{\beta}{\| \bar{\boldsymbol{\sigma}}^T \|} E \, \mathbf{1}_{\bar{\boldsymbol{\sigma}}^T} : \triangle\boldsymbol{\varepsilon}$$

Compute a trial effective stress $\hat{\bar{\boldsymbol{\sigma}}} = \alpha \, \bar{\boldsymbol{\sigma}}^T$. GO TO step (5).

NO: No plasticity exist. Set $\bar{\boldsymbol{\sigma}}_{t+\triangle t} = \bar{\boldsymbol{\sigma}}^T$. EXIT.

(5) Perform splitting of $\hat{\bar{\boldsymbol{\sigma}}}$ and calculate $\bar{\tau}^-(\hat{\bar{\boldsymbol{\sigma}}})$, according to (2.23). Check for $\bar{\tau}^- > r_t^-$?

YES: $H(\dot{d}^-_{t+\triangle t}) = 1$, plasticity and compressive damage exist, and so $\bar{\boldsymbol{\sigma}}_{t+\triangle t} = \hat{\bar{\boldsymbol{\sigma}}}$. EXIT.

NO: $H(\dot{d}^-_{t+\triangle t}) = 0$, no plasticity and no compressive damage evolution exist. So, $\alpha = 1$ and $\bar{\boldsymbol{\sigma}}_{t+\triangle t} = \bar{\boldsymbol{\sigma}}^T$. EXIT.

Box 2.2 – Algorithm for plastic-damage constitutive law

INPUT: A^+, r_0^+, r_t^+, A^-, B^-, r_0^-, r_t^-, $\mathbf{D_0}$, D_0^{-1}, K, β, E, $\bar{\boldsymbol{\sigma}}_t$, $\triangle\boldsymbol{\epsilon}$

OUTPUT: $\boldsymbol{\sigma}_{t+\triangle t}$, $r^+_{t+\triangle t}$, $r^-_{t+\triangle t}$, $d^+_{t+\triangle t}$, $d^-_{t+\triangle t}$

ALGORITHM:

(1) If $t = 0$ set

$$r_t^+ = r_0^+$$
$$r_t^- = r_0^-$$

(2) Evaluate $\bar{\boldsymbol{\sigma}}_{t+\triangle t}$ according to the procedure described in Box 2.1.

(3) Extract eigenvalues from $\bar{\boldsymbol{\sigma}}_{t+\triangle t}$ and split into $\bar{\boldsymbol{\sigma}}^+_{t+\triangle t}$ and $\bar{\boldsymbol{\sigma}}^-_{t+\triangle t}$ contributions. Evaluate $\bar{\sigma}^-_{oct_{t+\triangle t}}$ and $\bar{\tau}^-_{oct_{t+\triangle t}}$.

(4) Compute the equivalent stresses

$$\bar{\tau}^+_{t+\triangle t} = \sqrt{\bar{\boldsymbol{\sigma}}^+_{t+\triangle t} : \mathbf{D_0}^{-1} : \bar{\boldsymbol{\sigma}}^+_{t+\triangle t}}$$
$$\bar{\tau}^-_{t+\triangle t} = \sqrt{\sqrt{3}\,\left(K\,\bar{\sigma}^-_{oct_{t+\triangle t}} + \bar{\tau}^-_{oct_{t+\triangle t}}\right)}$$

(5) Evaluate damage variables

$$d^+_{t+\triangle t} = G^+(\bar{\tau}^+_{t+\triangle t})$$
$$d^-_{t+\triangle t} = G^-(\bar{\tau}^-_{t+\triangle t})$$

and update thresholds

$$r^+_{t+\triangle t} = max\left\{r^+_t,\ \bar{\tau}^+_{t+\triangle t}\right\}$$
$$r^-_{t+\triangle t} = max\left\{r^-_t,\ \bar{\tau}^-_{t+\triangle t}\right\}$$

(6) Compute the final Cauchy stress tensor:

$$\boldsymbol{\sigma}_{t+\triangle t} = (1 - d^+_{t+\triangle t})\,\bar{\boldsymbol{\sigma}}^+_{t+\triangle t} + (1 - d^-_{t+\triangle t})\,\bar{\boldsymbol{\sigma}}^-_{t+\triangle t}$$

2.10 – Numerical integration of constitutive law

In section 2.9 a special care was devoted to the explanation of the procedure for evaluating internal variables. It was emphasized that as soon as the strain tensor $\boldsymbol{\varepsilon}$ and its increment $\triangle\boldsymbol{\varepsilon}$ are determined, computation of updated variables d^+, d^- and $\boldsymbol{\varepsilon}^p$ can be performed by means of an almost closed-form algorithm. This feature is in fact of capital importance in the context of the present material model, ensuring large scale computations to be feasible, because almost no iterations are needed to evaluate the Cauchy stress tensor $\boldsymbol{\sigma}$ corresponding to a given strain tensor $\boldsymbol{\varepsilon}$.

For a global understanding of the plastic-damage algorithm, Box 2.2 schematizes all the operations needed for evaluating the Cauchy stress tensor. A remark is made for the extreme clearity and readability of the overall algorithm, as well for the simplicity of the involved operations.

2.11 – Numerical applications

2.11.1 – Tension-compression cyclic test

In order to check for the performance of the present plastic-damage constitutive law in a cyclic test, figure 2.2 shows the response of an idealized concrete specimen with the following properties[‡]:

$$
\begin{aligned}
E &= 20\ GPa \\
G_f &= 200\ J/m^2 \\
f_u^+ &= 1\ MPa \\
f_0^+ &= 1\ MPa \\
f_u^- &= 2\ MPa \\
f_0^- &= 1\ MPa \\
\beta &= 0.15
\end{aligned}
$$

‡ Selection of these properties was only oriented by didactic representation demands, avoiding the usual 1:10 ratios for concrete strengths under tensile and compressive loadings, which would almost preclude tensile domain in a small drawing.

(f_u^+ and f_u^- are tensile and compressive peak strengths, f_0^+ and f_0^- are tensile and compressive linear-elastic stress thresholds and G_f is the tensile fracture energy).

A complex loading scheme was imposed, firstly comprising an incursion into tensile regimen, up to the initial elastic threshold (point A), and followed by continuous damage until point B is attained; thereafter unloading takes place, with a return to point O, and then an incursion into compressive regimen is initiated. Up to the initial compressive threshold (point C) a linear-elastic behavior is obtained, but further loading induces progressive damage and plastic deformation; at point D compressive unloading is initiated and at point E reloading in tension takes place. Between points F and G further tensile damage occurs. At point G a second tensile unloading is induced, with reloading in compression up to point D; the path observed is represented by the broken line G-E-D. From point D a second reloading in compression is induced.

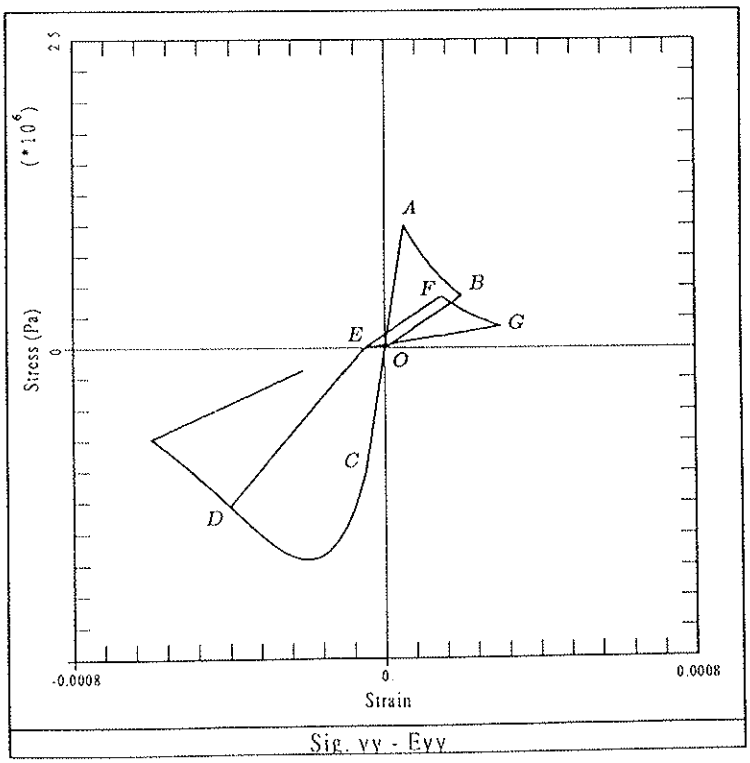

Figure 2.2 – Cyclic behavior of plastic-damage model

A detailed analysis of figure 2.2 allows to conclude that:

(1) The proposed model is able to reproduce the softening behavior in tension, as well the hardening and softening compressive behavior of concrete, accordingly to observational evidence.

(2) During path O-A-B, an initially undamaged material experiments tensile loads for the first time, exhibiting linear-elastic behavior up to tensile threshold (in this example the tensile peak strength, represented by point A) and a nonlinear behavior thereafter, which is evidenced by the branch A-B and by the damaged elastic modulus that is observed during discharge B-O. This shows that material has suffered an irreversible tensile damage.

(3) An incursion into tensile regimen without previous induced compressive damage does not enable any kind of plastic deformation to take place, as it is evidenced by the return to the origin O during the first tensile discharge (straight line B-O). This is obviously a direct consequence of the proposed model for plasticity (equation (2.33)), where irreversible deformations were supposed to be consequence of a phenomenon linked to compressive damage. As in this first phase of loading $H(\dot{d}^-) = 0$, no plastic strains will be observed upon unloading.

(4) When passing from tensile unloading to first compressive loading material model exhibits stiffness recovering: the elastic-damaged modulus changes from the damaged one in tension to the undamaged elastic in compression, as previous damage in tension is supposed to have no effect in material compressive behavior. This is a first evidence of the unilateral effect and of the memory capability of the present model.

(5) Straining in compression induces nonlinear behavior as soon as compressive threshold is overtaken. Unloading at point D shows that concrete has experienced damage (evidenced by the secant modulus associated to the straight line D-E) and plastic deformations (point E is no longer coincident with the origin O).

(6) When passing from compressive unloading to tensile reloading the unilateral effect is clearly observed, with the model exhibiting different damaged modulus during compressive unloading and tensile reloading. Furthermore, model recovers exactly the previous tensile damaged modulus (see that lines E-F and O-B are parallel) and has capability for maintaining the plastic deformations induced during compressive damaging: it is clear that the remaining tensile curve is shiffted along

the strain axis, which is precisely the induced plastic strain effect.

(7) During reloading in tensile domain the previous stress threshold (point F) is obeyed, which seems a physically realistic demand.

(8) Unloading at point G reveals that further damage has occurred in tension, but with no plastic strain evolution, as it is evidenced by discharge curve G-E.

(9) Reloading in compression reveals recovering of compressive damaged modulus (inclination of tensile unloading curve G-E is different from inclination of compressive reloading curve E-D) up to the previous compressive stress threshold. Further straining induces furher damage and plasticity.

From what was observed in figure 2.2, although with a simple and elegant formalism, the present model gives a physically realistic representation of the intended features of concrete, and satisfies the basic rate-independent requisits specified in section 1.2.

2.11.2 – Unidimensional cyclic compressive test

The ability of the proposed plastic-damage model for reproducing the observed behavior of a concrete specimen under cyclic uniaxial compressive loading can be checked by means of figure 2.3, where an experimental test taken from the reference Sinha *et al* (1964) (dotted line) is plotted against the response predicted by the numerical model (solid line).

The following concrete properties were considered:

$$E = 25\ GPa$$
$$f_u^- = 30\ MPa$$
$$f_0^- = 20\ MPa$$
$$\beta = 0.685$$

As it can be observed, predicted response reveals a fairly good agreement with the experimental test, namely in what concerns:

(1) the overall nonlinear behavior evidenced by the calculated envelope curve, either in the hardening or in the softening regimens, which is rather close to the test one;

(2) the residual plastic strain upon unloading, which is continuously increasing as further straining takes place, in accordance with the observed experimental behavior;

(3) the progressive degradation of the secant modulus, expressing that continuous damage is occurring, which reproduces rather well the the "average" lines from the test unloading-reloading loops.

Comparison between observed and predicted model responses puts into evidence that the selected compressive evolution laws, both for damage and for plasticity, are physically realistic and adequate for modelling the compressive behavior of a concrete specimen under uniaxial cyclic test.

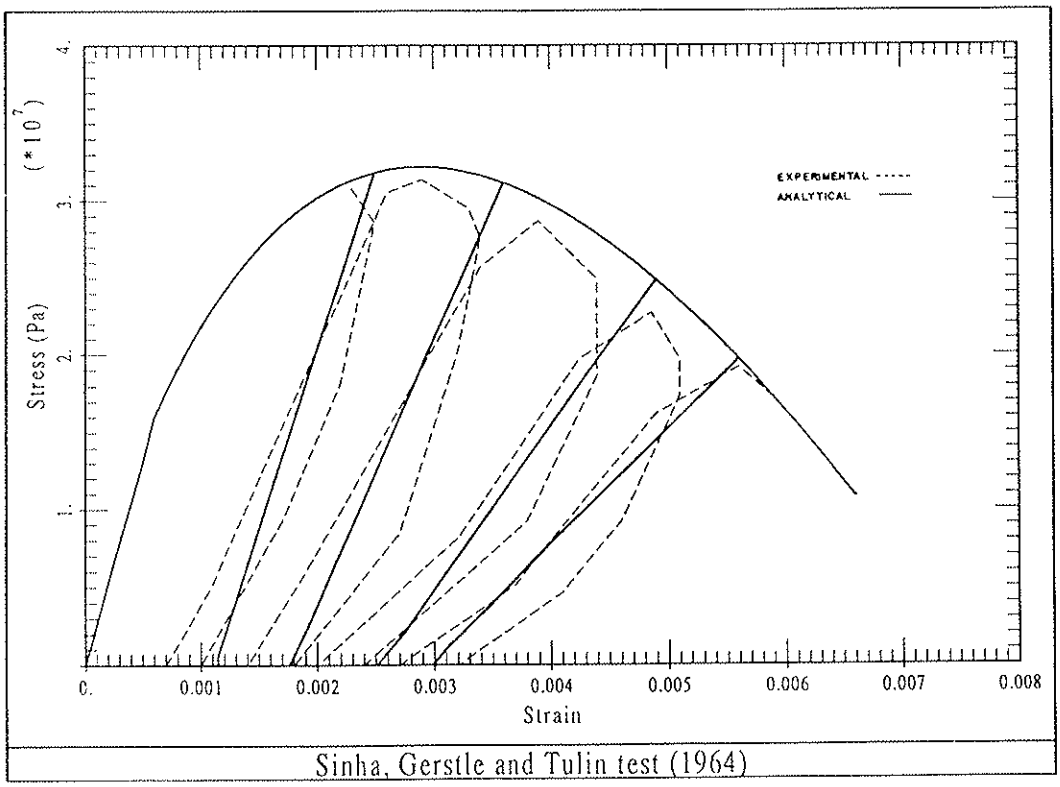

Figure 2.3 – Observed and predicted 1D compressive behavior

2.11.3 – Bidimensional compressive test

Having checked for the performance of the plastic-damage model under 1D conditions, a set of 2D experimental tests performed by Kupfer *et al* (1969) are plotted in figure 2.4.

A concrete specimen with the properties

$$\begin{aligned} E &= 31\ GPa \\ \nu &= 0.2 \\ f_u^- &= 32\ MPa \\ f_0^- &= 10\ MPa \\ \beta &= 0.318 \end{aligned}$$

is submmited to three different plane stress loading conditions, in which the pure normal stresses acting on its faces satisfy the following proportions:

$$\begin{aligned} (i) \qquad & \sigma_1 = 0, \quad \sigma_3/\sigma_2 = -1/0 \\ (ii) \qquad & \sigma_1 = 0, \quad \sigma_3/\sigma_2 = -1/-1 \\ (iii) \qquad & \sigma_1 = 0, \quad \sigma_3/\sigma_2 = -1/-0.52 \end{aligned}$$

Solid lines refer to numerical model predictions and dotted lines correspond to the observed experimental behavior.

As it can be noticed, the plastic-damage model captures satisfactorily the overall experimental behavior, specially taking into consideration the purposes intended within the context of large scale computations, and the simplifications which had to be introduced in order to obtain an almost closed-form algorithm. Test and model curves exhibit an acceptable separation.

Note also that in figure 2.5, where representation of σ_3/ε_2 curves are plotted for the same concrete experiment, the numerical predictions are less accurate than the ones in figure 2.4. This is consequence of the inability of the proposed simplified plastic model to account for plastic deformations along direction defined by stress σ_1, where a null effective stress component exists, hence inducing a null plastic strain. Anyway, this limitation must be regarded as not a serious one, because by one side it was foreseeable, due to the particular form attributed in equation (2.33) to the evolution of plastic

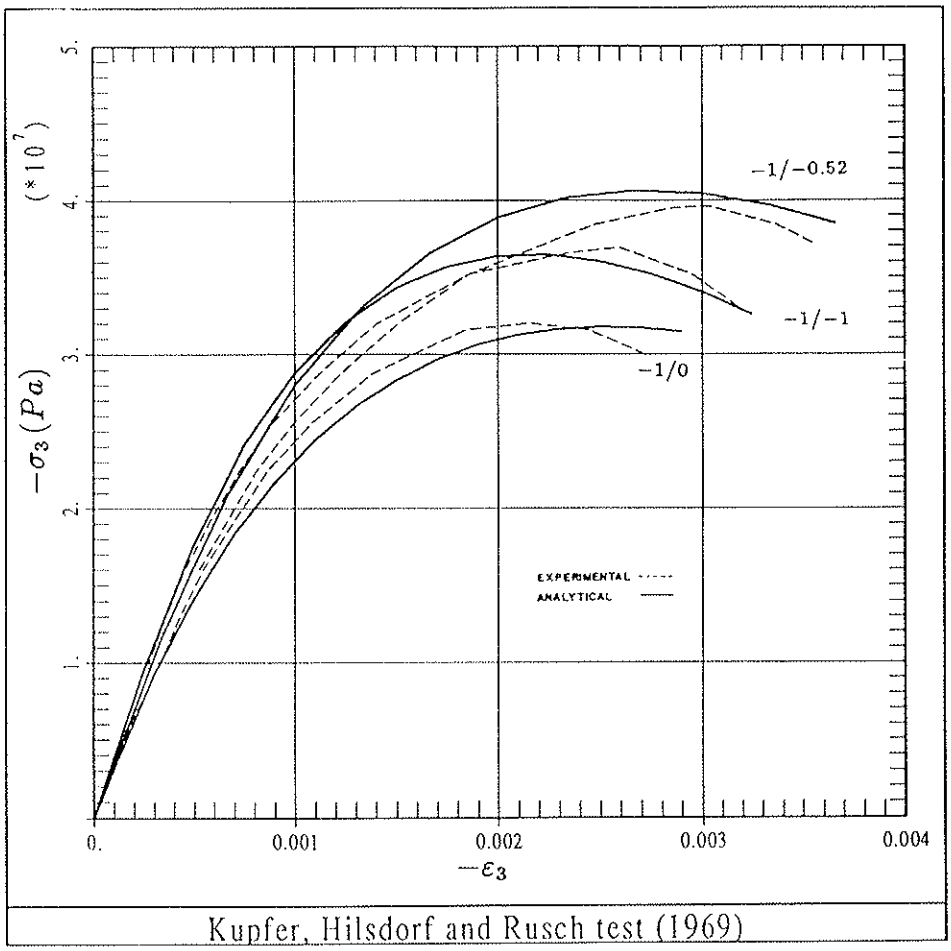

Figure 2.4 – Observed and predicted 2D σ_3/ε_3 compressive behavior

strain tensor, and by other side plasticity is mainly intended as an overall effect, inducing global deformation irreversibility and dissipation of plastic energy (important to account for structural damping).

An important feature of the present constitutive law, which is clearly visible in figure 2.4, is its ability for predicting the concrete strength enhancement under 2D compressive loading, in accordance with observed macroscopic behavior (note that in figure 2.4 observed and predicted peak strengths are almost identical), which constitutes a remarkable advance when compared to other versions of similar concrete damage models (where concrete strength under biaxial compression is decreased with reference to the one observed in uniaxial tests (Mazars and Pijaudier-Cabot (1989), Suaris *et al* (1990)).

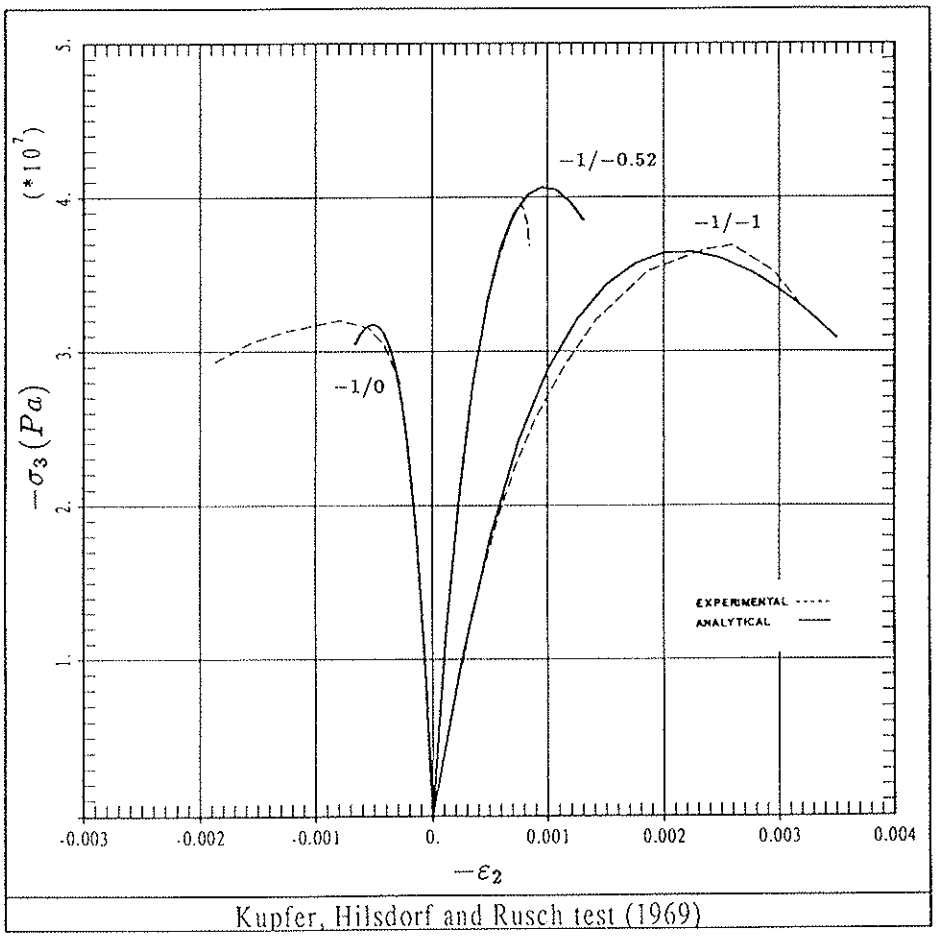

Figure 2.5 – Observed and predicted 2D σ_3/ϵ_2 compressive behavior

2.11.4 – Tridimensional compressive test

As a final benchmark test, figure 2.6 presents a comparison between predictions obtained by means of the present plastic-damage model and the experimental results respecting to a concrete tridimensional test (Green and Swanson (1973)). The test was performed applying an increasing normal stress along the specimen vertical axis and three different sets of constant normal confining stresses along the horizontal directions, with values 0.0 MPa, 6.895 MPa or 13.79 MPa respectively.

The following properties were considered for concrete:

$$E = 41.37\ GPa$$
$$\nu = 0.2$$
$$f_u^- = 48\ MPa$$
$$f_0^- = 10\ MPa$$
$$\beta = 0$$

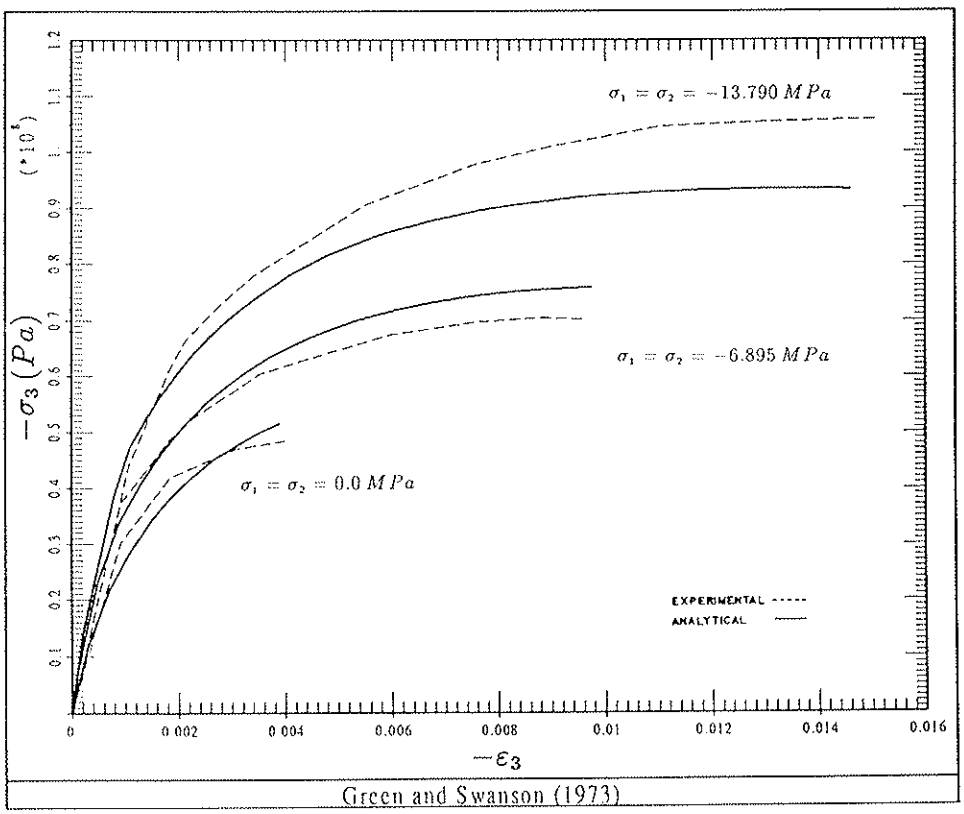

Figure 2.6 – Observed and predicted 3D behavior

From observation of figure 2.6 it can be concluded that the proposed plastic-damage model captures satisfactorily the observed strength enhancement due to the tridimensional confinement. Furthermore, the predicted increasing ductility of concrete is in satisfactory accordance with

the experimental one, as well the overall response curves, whose deviations can be considered acceptable keeping in mind the computations intended with the present model[‡].

2.12 – Final remarks

The experimental tests which have been presented show that the proposed model is able to predict the nonlinear inviscid material behavior in a wide range of situations, covering unidimensional, bidimensional and tridimensional applications.

- Plasticity is accounted in a simplified but elegant fashion, and the stiffness degradation due to damage is fully captured.

- The softening associated to tensile loading as well the hardening and softening characteristics evidenced by concrete under compressive loading are also captured by the numerical model.

- Stiffness recovering when passing from tension to compression (or *vice-versa*) is easily attended by the plastic-damage model, due to the internal "memories" associated to the independent damage variables for tension and compression. The unilateral effect is hence adequately modelled.

- Strength enhancement under monotonic biaxial and triaxial loading is also taken into account, in reasonable agreement with experimental evidence.

From the performance of the proposed model it is concluded that it satisfies the basic rate-independent requisits which were defined in section 1.2, rendering an efficient and economical algorithm, with a physical background, which permits to obtain realistic informations about material (and structural) behavior.

---

‡ Or even negligible when compared to other sources of uncertainties of major and not quantifiable order of magnitude, as it is the case of the open issue respecting the seismic input characterization.

Chapter 3

EXTENSION OF PLASTIC-DAMAGE MODEL TO ACCOUNT FOR RATE DEPENDENCY

3.1 – General aspects

As referred in Chapter 1, concrete exhibits a rate dependent behavior when submmited to high speed straining (see figure 1.5), whose visible effects are the significant increase of dynamic strengths and the decrease of nonlinearity on the stress-strain response curves (see figure 3.1), when compared to what is observed on static tests.

This peculiar behavior is rather important under impulsive loading, as it occurs when structures are subjected to impacts or explosions, where straining rates $\dot{\varepsilon} > 10^{-2}/s$ (Chappuis (1987)) can be observed, but the phenomenon is already important in the "impulsive restraint fatigue domain", at which category belongs the earthquake loading, with rates of straining within the interval $10^{-6}/s < \dot{\varepsilon} < 10^{-1}/s$. As it can be observed in figure 1.5, dynamic strength can be enhanced, with respect to the static one, up to 80 % in tension and 25 % in compression, for the "impulsive restraint fatigue domain".

Observational experience shows that rate sensitivity is mainly due to the fact that growth of internal microcracking (for a particular level of strain) is retarded at high strain rates (Suaris and Shah (1984)). Being known that for concrete (and other geomaterials) damage is essentially due to the nucleation and growth of microvoids and microcracks, it is comprehensible that a diminuishing of microcracking with increasing strain rate will induce a reduction in macroscopic nonlinear behavior, and an increase of dynamic strengths.

The importance of this observed phenomenon has already been recognized long time ago, and attemps were made for the constitutive laws to be able to account for it. However, its complexity and the need for some

sophistication in the numerical models precluded it from common usage, the customary practice being to account for rate sensitivity by means of empirical formulas and drastic simplifying assumptions.

Contributions from viscoplasticity were some of the first attemps to deal with rate dependency with theoretical consistency. Among others, Bićanić and Zienkiewicz (1983) proposed one of these models, with similarity to the "bounding-surface" concept.

More recently, important experimental and theoretical contributions have been introduced by Suaris *et al* ((1983), (1984), (1985), (1990)), which provided scientific tools for dealing with this phenomenon in a realistic manner. Starting from the observed evidence that this particular behavior is in fact consequence of the above described strain-rate dependency of the internal damage evolution, they proposed a material model based on the Continuum Damage Mechanics (Suaris and Shah (1985)), with a vectorial representation for the internal damage, the evolution of which being governed by a linear differential equation of second-order, accounting for the "microcrack inertia effect".

It is obvious that for the purposes intended by the present work‡ an algorithm should evolve from the previous plastic-damage version, keeping its closed-form nature as much as possible. Due to the coupling between nonlinear rate-sensitivity and damage, the appropriate environment for dealing with this strain-dependency is the Continuum Damage Mechanics, yet with an easier formalism than the above cited sophisticated one from Suaris and Shah (1985), in order to obtain high algorithmic efficiency.

In this chapter an extension will be introduced into the plastic-damage model, by considering a viscous regularization of the rate-independent damage evoution laws defined through equations (2.26-2.27), following a procedure inspired in a viscous-damage model from Simo and Ju (1987a-b).

3.2 – Viscous-damage evolution laws

With a reasoning similar to the classical Perzina viscoplastic regularization, Simo and Ju (1987a) proposed an evolution law for an internal damage variable which had the following features:

‡ It must be reminded that the scope of the present work is to capture the seismic behavior of large-scale concrete structures, the emphasys being mainly on capturing overall (or global) structural effects, excluding excessive detail at local level.

(i) a damage fluidity parameter ϑ is introduced, supposed to be a material property;

(ii) with an infinity value for this parameter, the rate-independent (or inviscid) damage evolution law is recovered;

(iii) with a zero value for ϑ, damage variable is prevented to have evolution, thus rendering an instantaneous elastic response.

Inspired on these considerations, and maintaining the previous decomposition into d^+ and d^- damage variables, the following evolution laws will the adopted in the present work:

- Tension

$$\dot{d}^+ = \frac{\vartheta^+}{(f_u^+)^{a^+/2}} \langle \bar{\tau}^+ - r^+ \rangle^{a^+} \frac{\partial G^+(\bar{\tau}^+)}{\partial \bar{\tau}^+} \tag{3.1a}$$

$$\dot{r}^+ = \frac{\vartheta^+}{(f_u^+)^{a^+/2}} \langle \bar{\tau}^+ - r^+ \rangle^{a^+} \tag{3.1b}$$

- Compression

$$\dot{d}^- = \frac{\vartheta^-}{(f_u^-)^{a^-/2}} \langle \bar{\tau}^- - r^- \rangle^{a^-} \frac{\partial G^-(\bar{\tau}^-)}{\partial \bar{\tau}^-} \tag{3.2a}$$

$$\dot{r}^- = \frac{\vartheta^-}{(f_u^-)^{a^-/2}} \langle \bar{\tau}^- - r^- \rangle^{a^-} \tag{3.2b}$$

where ϑ^+, ϑ^- are the concrete fluidity parameters associated to tensile and compressive damage mechanisms, and a^+, a^- are positive exponents. All of these parameters are supposed to be material properties, the determination of which being performed by means of uniaxial tensile and compressive tests. Note that the separeted values which can be attributed to these tensile or compressive parameters and exponents will permit to account for the distinct concrete rate sensitivities (greater under tensile than under compressive loading).

3.3 – Thermodynamics and dissipation

The changes introduced into plastic-damage model to account for rate dependency are limited to the particular forms attributed to damage evolution laws (3.1) and (3.2). Considerations performed on Chapter 2 around thermodynamic dissipation remain absolutely valid for the present plastic-viscous-damage model, because for ensuring positive dissipation the

only demand from damage evolution laws is that they have to satisfy the following conditions[‡]:

$$\dot{d}^+ \geq 0$$

$$\dot{d}^- \geq 0$$

Inspection of equations (3.1a) and (3.2a) enables to conclude that non-decreasing damage variables are obtained, hence automatically satisfying condition of dissipation.

For the Cauchy stress tensor, equation (2.55) keeps absolute validity for the present extension, that is:

$$\boldsymbol{\sigma} = (1 - d^+)\, \bar{\boldsymbol{\sigma}}^+ + (1 - d^-)\, \bar{\boldsymbol{\sigma}}^- \tag{3.3}$$

3.4 – Computation of thresholds and damage variables

For evaluating damage variables and damage thresholds, a numerical algorithm needs to be implemented, preferably with the most closed-form structure as possible. For didactic reasons presentation will be made only for tensile variables, although an interily analogous scheme applies for compressive damage variable and threshold.

Defining auxiliar variables ϑ_*^+ and c^+, such that

$$\vartheta_*^+ = \frac{\vartheta^+}{(f_u^+)^{a^+/2}} \tag{3.4}$$

$$c^+ = \frac{\partial G^+(\bar{\tau}^+)}{\partial \bar{\tau}^+} \tag{3.5}$$

and adopting a backward-Euler difference scheme for integrating equations (3.1a, 3.1b), the equivalent stress threshold and its correspondent damage variable can be evaluated for the instant $t + \Delta t$ according to the following expressions (recall of notation defined for equation (2.71) is made once more):

$$r_{t+\Delta t}^+ = r_t^+ + \Delta t\, \vartheta_*^+ \left\langle \bar{\tau}_{t+\Delta t}^+ - r_{t+\Delta t}^+ \right\rangle^{a^+} \tag{3.6}$$

[‡] Obviously, it is already supposed that

$$0 \leq d^+ \leq 1$$
$$0 \leq d^- \leq 1$$

owing to the intrinsic concept of damage variables.

$$d^+_{t+\Delta t} = d^+_t + \Delta t\, \vartheta^+_* \left\langle \bar{\tau}^+_{t+\Delta t} - r^+_{t+\Delta t} \right\rangle^{a^+} c^+_{t+\Delta t} \tag{3.7}$$

The analysis of the algorithmic expression (3.7) puts into evidence that computation of $d^+_{t+\Delta t}$ becomes an easy task after threshold $r^+_{t+\Delta t}$ have been updated. In fact, $\bar{\tau}^+_{t+\Delta t}$ and $c^+_{t+\Delta t}$ are easily calculated because they strictly depend on the effective stress tensor $\bar{\boldsymbol{\sigma}}^+_{t+\Delta t}$ (which is supposed to have already been updated according to the procedure described on Box 2.1), and the other entities present on equation (3.7) are known at the beginning of step $t + \Delta t$.

So, the real numerical problem to be solved is the determination of $r^+_{t+\Delta t}$, which according to the nonlinear equation (3.6) can be performed by means of an explicit procedure only if exponent a^+ is an integer not greater than 4 (at Simo and Ju (1987a) an exponent equal to 1 was used), in which case mathematical solutions exist. However, in the present work it has been observed that best fitting with concrete experimental tests is obtained if greater exponents are adopted, which leads to high-order equations, without known theoretical solutions. An iterative scheme must hence be introduced for updating r^+ ; anyway, the operations needed for iterating are very elemental, and by means of a Newton-Raphson method a fast rate of convergence is obtained for the threshold updating solver.

3.4.1 – Thresholds updating

Considering the Newton-Raphson method for the x root-finding of equation $f(x) = 0$, an iterative algorithm of the form (Burden and Faires (1985)):

$$x_{i+1} = x_i - \frac{f(x_i)}{f'(x_i)} \tag{3.8}$$

can be set, with x_{i+1} being the $(i+1)$-th improved approximation to the exact root x, x_i the previous (i)-th approximation, and with f' denoting the first derivative of f.

Rearranging equation (3.6) and performing elemental mathematics, it will be possible to define:

$$f^+\left(r^+_{t+\Delta t}\right) = -r^+_{t+\Delta t} + r^+_t + \Delta t\, \vartheta^+_* \left\langle \bar{\tau}^+_{t+\Delta t} - r^+_{t+\Delta t} \right\rangle^{a^+} \tag{3.9}$$

$$\left(f^+\right)'\left(r^+_{t+\Delta t}\right) = -1 - a^+ \Delta t\, \vartheta^+_* \left\langle \bar{\tau}^+_{t+\Delta t} - r^+_{t+\Delta t} \right\rangle^{(a^+-1)} \tag{3.10}$$

Box 3.1 – Algorithm for updating of thresholds and damage variables on rate-dependent model (substitutes item (5) at Box 2.2)

INPUT:

$\vartheta_*^+,\ \vartheta_*^-,\ a^+,\ a^-,\ \bar{r}_{t+\Delta t}^+,\ \bar{r}_{t+\Delta t}^-,\ c_{t+\Delta t}^+,\ c_{t+\Delta t}^-,\ r_t^+,\ r_t^-,\ d_t^+,\ d_t^-,\ \Delta t, TOLER$

OUTPUT:

$r_{t+\Delta t}^+,\ r_{t+\Delta t}^-,\ d_{t+\Delta t}^+,\ d_{t+\Delta t}^-$

ALGORITHM:

(1) Set

$$\begin{aligned} i &= 0 \\ \left(r_{t+\Delta t}^+\right)_i &= r_t^+ \\ \left(r_{t+\Delta t}^-\right)_i &= r_t^- \end{aligned}$$

(2) Evaluate $f^+,\ (f^+)',\ f^-,\ (f^-)'$ according to (3.9) and (3.10).

(3) Evaluate $\left(r_{t+\Delta t}^+\right)_{i+1}$ and $\left(r_{t+\Delta t}^-\right)_{i+1}$ according to (3.11).

(4) Evaluate the errors

$$\begin{aligned} error^+ &= \frac{\left(r_{t+\Delta t}^+\right)_{i+1} - \left(r_{t+\Delta t}^+\right)_i}{\left(r_{t+\Delta t}^+\right)_{i+1}} \\ error^- &= \frac{\left(r_{t+\Delta t}^-\right)_{i+1} - \left(r_{t+\Delta t}^-\right)_i}{\left(r_{t+\Delta t}^-\right)_{i+1}} \end{aligned}$$

(5) Check for convergence: $|error^+|,\ |error^-| \leq TOLER$?

YES: Convergence attained. Set

$$\begin{aligned} r_{t+\Delta t}^+ &= \left(r_{t+\Delta t}^+\right)_{i+1} \\ r_{t+\Delta t}^- &= \left(r_{t+\Delta t}^-\right)_{i+1} \end{aligned}$$

and GO TO step (6).

Box 3.1 – (continuation)

NO: Further iteration needed. Set

$$i = i + 1$$

and GO TO step (2).

(6) Update damage variables

$$d^+_{t+\Delta t} = d^+_t + \Delta t\, \vartheta^+_* \left\langle \bar{\tau}^+_{t+\Delta t} - r^+_{t+\Delta t} \right\rangle^{a^+} c^+_{t+\Delta t}$$

$$d^-_{t+\Delta t} = d^-_t + \Delta t\, \vartheta^-_* \left\langle \bar{\tau}^-_{t+\Delta t} - r^-_{t+\Delta t} \right\rangle^{a^-} c^-_{t+\Delta t}$$

So, the sequence of improved approximations to $r^+_{t+\Delta t}$ can be obtained according to

$$\left(r^+_{t+\Delta t}\right)_{i+1} = \left(r^+_{t+\Delta t}\right)_i - \frac{f^+\left(\left(r^+_{t+\Delta t}\right)_i\right)}{(f^+)'\left(\left(r^+_{t+\Delta t}\right)_i\right)} \tag{3.11}$$

which together with a convergence criterion will permit to update threshold $r^+_{t+\Delta t}$.

3.4.2 – Numerical integration of constitutive law

In Box 2.2 (Chapter 2) the algorithmic procedure for implementing the rate-independent constitutive law was defined. Except for item (5), devoted to the evaluation of thresholds and damage variables, its structure remains valid for the present rate-dependent extension, only being necessary to detail the referred updating of r^+, r^-, d^+ and d^-, which is performed at Box 3.1.

3.5 – Some limit situations

Numerical procedure defined by equation (3.7) can be derived to obtain the algorithmic rate $\dot{d}^+_{t+\Delta t}$. Keeping in mind that

$$\dot{d}_{t+\Delta t} = \frac{\partial\, d_{t+\Delta t}}{\partial\, \boldsymbol{\varepsilon}_{t+\Delta t}} \cdot \dot{\boldsymbol{\varepsilon}}_{t+\Delta t} \tag{3.12}$$

it is possible to state

$$\dot{d}^+_{t+\Delta t} = a^+ \Delta t \, \vartheta^+_* \left\langle \bar{\tau}^+_{t+\Delta t} - r^+_{t+\Delta t} \right\rangle^{(a^+-1)} c^+_{t+\Delta t} \frac{\partial \left(\bar{\tau}^+_{t+\Delta t} - r^+_{t+\Delta t} \right)}{\partial \boldsymbol{\varepsilon}_{t+\Delta t}} \cdot \dot{\boldsymbol{\varepsilon}}_{t+\Delta t} +$$

$$+ \Delta t \, \vartheta^+_* \left\langle \bar{\tau}^+_{t+\Delta t} - r^+_{t+\Delta t} \right\rangle^{a^+} \frac{\partial c^+_{t+\Delta t}}{\partial \boldsymbol{\varepsilon}_{t+\Delta t}} \cdot \dot{\boldsymbol{\varepsilon}}_{t+\Delta t} \tag{3.13}$$

Performing further mathematics, terms envolving derivatives can assume the following aspect:

$$\frac{\partial \left(\bar{\tau}^+_{t+\Delta t} - r^+_{t+\Delta t} \right)}{\partial \boldsymbol{\varepsilon}_{t+\Delta t}} \cdot \dot{\boldsymbol{\varepsilon}}_{t+\Delta t} = \frac{\partial \bar{\tau}^+_{t+\Delta t}}{\partial \boldsymbol{\varepsilon}_{t+\Delta t}} \cdot \dot{\boldsymbol{\varepsilon}}_{t+\Delta t} - \frac{\partial r^+_{t+\Delta t}}{\partial \boldsymbol{\varepsilon}_{t+\Delta t}} \cdot \dot{\boldsymbol{\varepsilon}}_{t+\Delta t} =$$

$$= \dot{\bar{\tau}}^+_{t+\Delta t} - \dot{r}^+_{t+\Delta t} \tag{3.14}$$

$$\frac{\partial c^+_{t+\Delta t}}{\partial \boldsymbol{\varepsilon}_{t+\Delta t}} \cdot \dot{\boldsymbol{\varepsilon}}_{t+\Delta t} = \frac{\partial c^+_{t+\Delta t}}{\partial \bar{\tau}^+_{t+\Delta t}} \frac{\partial \bar{\tau}^+_{t+\Delta t}}{\partial \boldsymbol{\varepsilon}_{t+\Delta t}} \cdot \dot{\boldsymbol{\varepsilon}}_{t+\Delta t} = \frac{\partial c^+_{t+\Delta t}}{\partial \bar{\tau}^+_{t+\Delta t}} \dot{\bar{\tau}}^+_{t+\Delta t} \tag{3.15}$$

Differentiating equation (3.6) with respect to time enables to express that

$$\dot{r}^+_{t+\Delta t} = a^+ \Delta t \, \vartheta^+_* \left\langle \bar{\tau}^+_{t+\Delta t} - r^+_{t+\Delta t} \right\rangle^{(a^+-1)} \left(\dot{\bar{\tau}}^+_{t+\Delta t} - \dot{r}^+_{t+\Delta t} \right) \tag{3.16}$$

and consequently

$$\dot{r}^+_{t+\Delta t} = \frac{a^+ \Delta t \, \vartheta^+_* \left\langle \bar{\tau}^+_{t+\Delta t} - r^+_{t+\Delta t} \right\rangle^{(a^+-1)}}{1 + a^+ \Delta t \, \vartheta^+_* \left\langle \bar{\tau}^+_{t+\Delta t} - r^+_{t+\Delta t} \right\rangle^{(a^+-1)}} \dot{\bar{\tau}}^+_{t+\Delta t} \tag{3.17}$$

Substituting this result into (3.14) and transforming equation (3.13) according to expressions (3.14) and (3.15) finally renders:

$$\dot{d}^+_{t+\Delta t} = \Delta t \, \vartheta^+_* \left\langle \bar{\tau}^+_{t+\Delta t} - r^+_{t+\Delta t} \right\rangle^{(a^+-1)} \left[\frac{a^+ c^+_{t+\Delta t}}{1 + a^+ \Delta t \, \vartheta^+_* \left\langle \bar{\tau}^+_{t+\Delta t} - r^+_{t+\Delta t} \right\rangle^{(a^+-1)}} + \right.$$

$$\left. + \left\langle \bar{\tau}^+_{t+\Delta t} - r^+_{t+\Delta t} \right\rangle \frac{\partial c^+_{t+\Delta t}}{\partial \bar{\tau}^+_{t+\Delta t}} \right] \dot{\bar{\tau}}^+_{t+\Delta t} \tag{3.18}$$

For compression a similar expression would be obtained:

$$\dot{d}^-_{t+\Delta t} = \Delta t \, \vartheta^-_* \left\langle \bar{\tau}^-_{t+\Delta t} - r^-_{t+\Delta t} \right\rangle^{(a^- -1)} \left[\frac{a^- c^-_{t+\Delta t}}{1 + a^- \Delta t \, \vartheta^-_* \left\langle \bar{\tau}^-_{t+\Delta t} - r^-_{t+\Delta t} \right\rangle^{(a^- -1)}} + \right.$$

$$\left. + \left\langle \bar{\tau}^-_{t+\Delta t} - r^-_{t+\Delta t} \right\rangle \frac{\partial c^-_{t+\Delta t}}{\partial \bar{\tau}^-_{t+\Delta t}} \right] \dot{\bar{\tau}}^-_{t+\Delta t} \tag{3.19}$$

Inspection of these expressions enables to conclude that:

(i) null values for ϑ^+ and ϑ^- ‡ impose that $\dot{d}^+$ and $\dot{d}^-$ are equal to zero, which means that damage evolution can not take place – this implies that an instantaneous linear-elastic solution is obtained;

(ii) ϑ^+ and ϑ^- approaching infinity will determine that damage rate (exemplifying only for tension) will tend to

$$\dot{d}^+_{t+\Delta t} \;\rightarrow\; c^+_{t+\Delta t}\,\dot{\bar{\tau}}^+_{t+\Delta t} + \Delta t\,\vartheta^+_*\,\langle \bar{\tau}^+_{t+\Delta t} - r^+_{t+\Delta t}\rangle^{a^+}\,\frac{\partial\, c^+_{t+\Delta t}}{\partial\, \bar{\tau}^+_{t+\Delta t}}\,\dot{\bar{\tau}}^+_{t+\Delta t}$$

in which the first additive term corresponds to the already obtained inviscid evolution law defined by equation (2.31). The second term is a spurious contribution due to the linearization which has been considered at equations (3.6) and (3.7), which will be cancelled as refinement is introduced, that is, as $\Delta t \rightarrow 0$. In this situation ($\vartheta^+ \rightarrow \infty$, $\Delta t \rightarrow 0$), the previous rate independent model is recovered (obviously an identical set of conclusions would be vallid for compression).

3.6 – Numerical applications

Performance of the proposed rate dependent algorithm will be evaluated with reference to a set of experimental tests performed by Suaris and Shah (1985), for a concrete with a Young's modulus E = 34 GPa. Concrete behavior was registered for two distinct sets of straining rates:

(i) a quasi-static one, with $\dot{\varepsilon} = 10^{-6}\,/s$, where rate dependency can be considered almost absent;

(ii) a very fast one, with $\dot{\varepsilon} = 1\,/s$ for tension and $\dot{\varepsilon} = 0.088\,/s$ for compression, where viscous effects have to be modelled. These straining rates can be considered an upper-limit for those which can be expected under earthquake loading.

---

‡ This is equivalent to set $\vartheta^+_* = 0$ and $\vartheta^-_* = 0$.

3.6.1 – Rate-dependent tensile test

In figure 3.1 the experimental results and the predictions from the present model can be compared, when concrete was submmitted to tensile loading. The following values have been adopted for the relevant model properties (set 1):

$$\alpha^+ = 7.0$$
$$\vartheta^+ = 2.15 \times 10^4$$
$$f_u^+ = 5.37\ MPa$$
$$f_0^+ = 3.00\ MPa$$

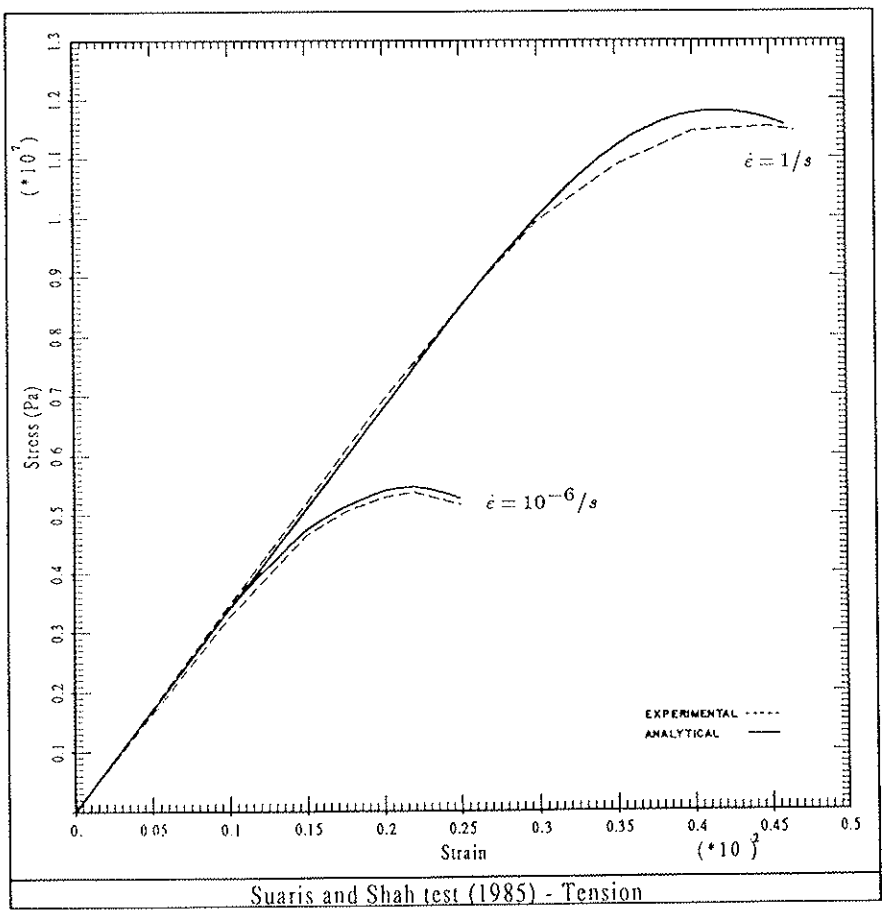

Figure 3.1 – Rate-dependent tensile results (set 1)

It can be observed that good approximation to the test results is obtained, with the predicted response curves having little deviation from the experimental ones.

However, the above considered α^+ exponent provided worse predictions for intermediate straining rates (not represented), with the material viscous model exhibiting a strong tendency to return to the rate independent situation. To circunvent this undesirable behavior higher exponents have to be considered, as for the case illustrated in figure 3.2, where the following parameters were used (set 2):

$$\alpha^+ = 8.0$$
$$\vartheta^+ = 4.99 \times 10^7$$

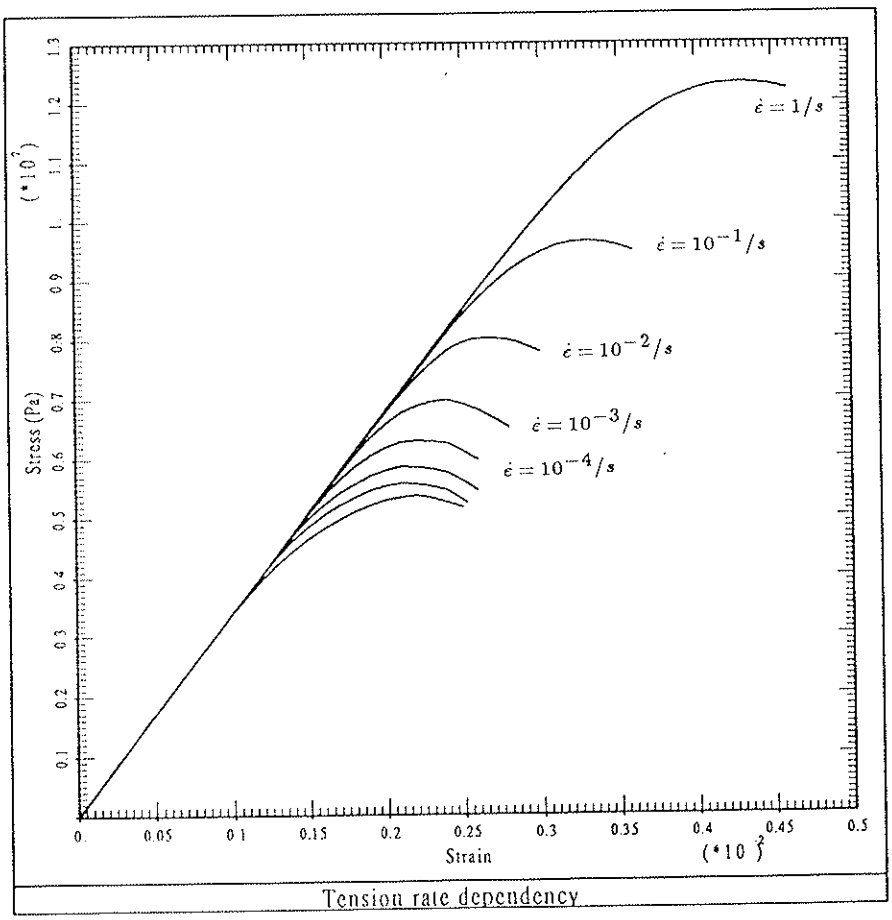

Figure 3.2 – Rate-dependent tensile results (set 2)

Now, it can be observed that numerical model exhibits a "smoother" performance, that is, dynamic strength grows continuously with increasing strain-rates, in accordance with what is experimentally observed. In this situation, predictions for the ratio

$$Ratio = \frac{Dynamic\,Strength}{Static\,Strength} \tag{3.20}$$

can be taken from the present model, which, as it can be seen on figure 3.5, are in excellent agreement with the experimental results from the reference Suaris and Shah (1985).

3.6.2 – Rate-dependent compressive test

Performing a similar set of predictions for compressive behavior, and adopting the following material properties (set 3):

$$\begin{aligned} \alpha^- &= 2.0 \\ \vartheta^- &= 936 \times 10^4 \\ f_u^- &= 46.80\ MPa \\ f_0^- &= 10.00\ MPa \end{aligned}$$

in figure 3.3 numerical and experimental results are compared. Once more it can be observed that good agreement is obtained.

However, with the selected parameters some underestimation of strength enhancement would be observed for strain-rates bellow $\dot{\varepsilon} = 0.088\,/s$ (the same phenomenon as for tensile test), reason by which another set of viscous parameters was selected (set 4):

$$\begin{aligned} \alpha^- &= 10.0 \\ \vartheta^- &= 8.98 \times 10^7 \end{aligned}$$

In figure 3.4 the obtained numerical results are plotted against the experimental observations. It can be observed that an overall accordance is obtained, namely in what concerns the peak strength predicted for $\dot{\varepsilon} = 0.088\,/s$, with the present constitutive law exhibiting some tendency for underestimating the peak deformations.

When the ratio defined by expression (3.20) is plotted both for experimental and numerical results (see figure 3.5), once more it is evident the ability of the proposed model to account for the phenomenon of compressive strength enhancement.

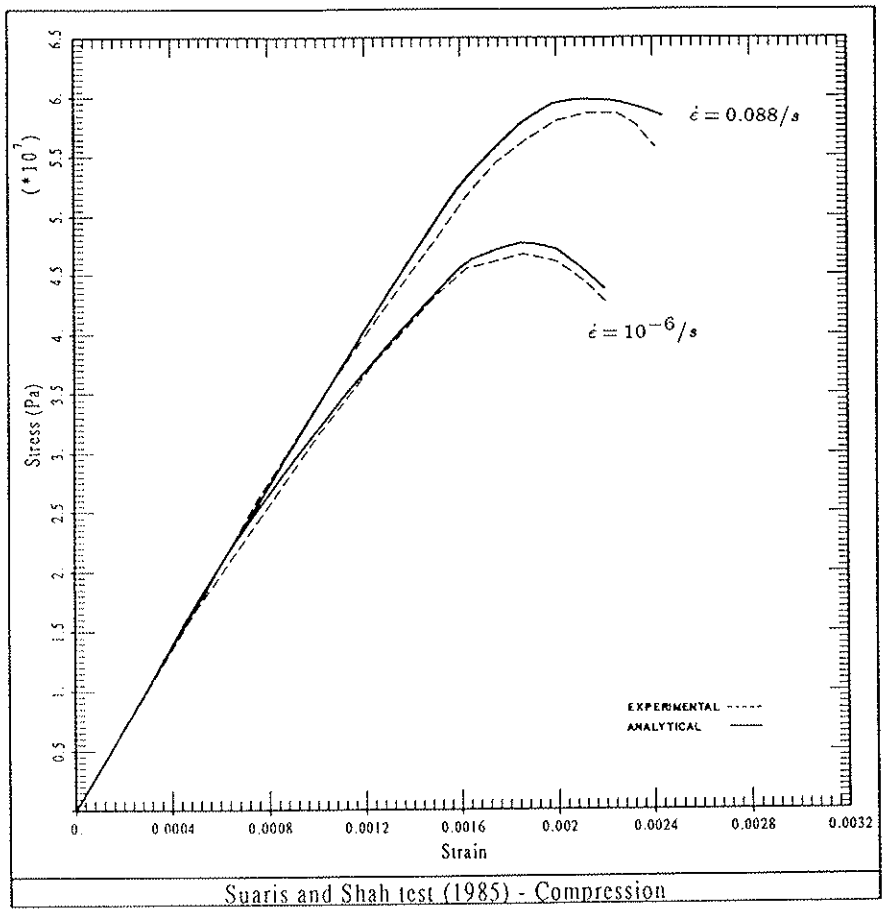

Figure 3.3 – Rate-dependent compressive results (set 3)

3.7 – Final remarks

The numerical applications which were performed by means of the plastic-viscous-damage concrete material model showed its good capability for full capturing the observed strength enhancement associated to increasing strain-rates, including the distinct rate dependency patterns exhibited under tensile and compressive loading.

Furthermore, predicted and experimental stress-strain curves showed a satisfactory accordance.

The present plastic-viscous-damage model provides a general formulation

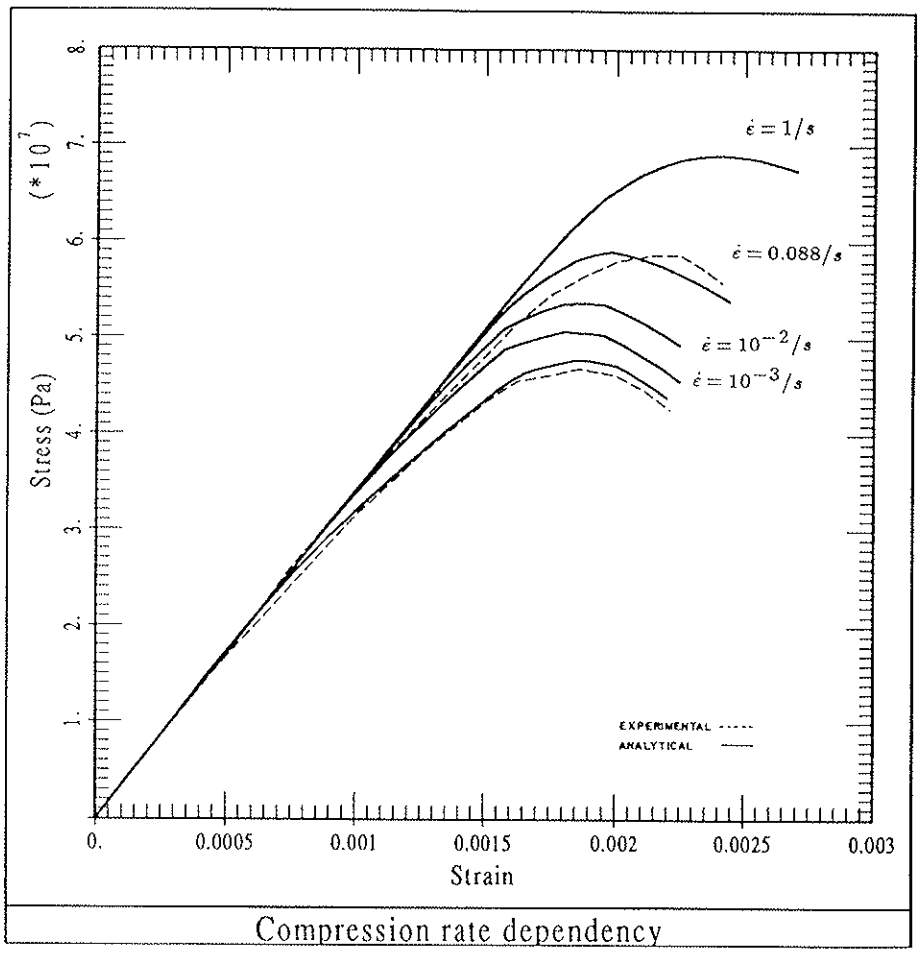

Figure 3.4 – Rate-dependent compressive results (set 4)

for the intended concrete constitutive law, enabling an hierarchical model approach to concrete behavior, that is: the elastic linearity, and the nonlinearity (comprizing damage and/or plasticity) considered on its versions with or without rate dependency. For so, only an appropriate choice has to be made for the material parameters.

In what concerns the algorithm itself, a rather robust numerical implementation is obtained, thus avoiding complex error-inducing and large time-consuming codes.

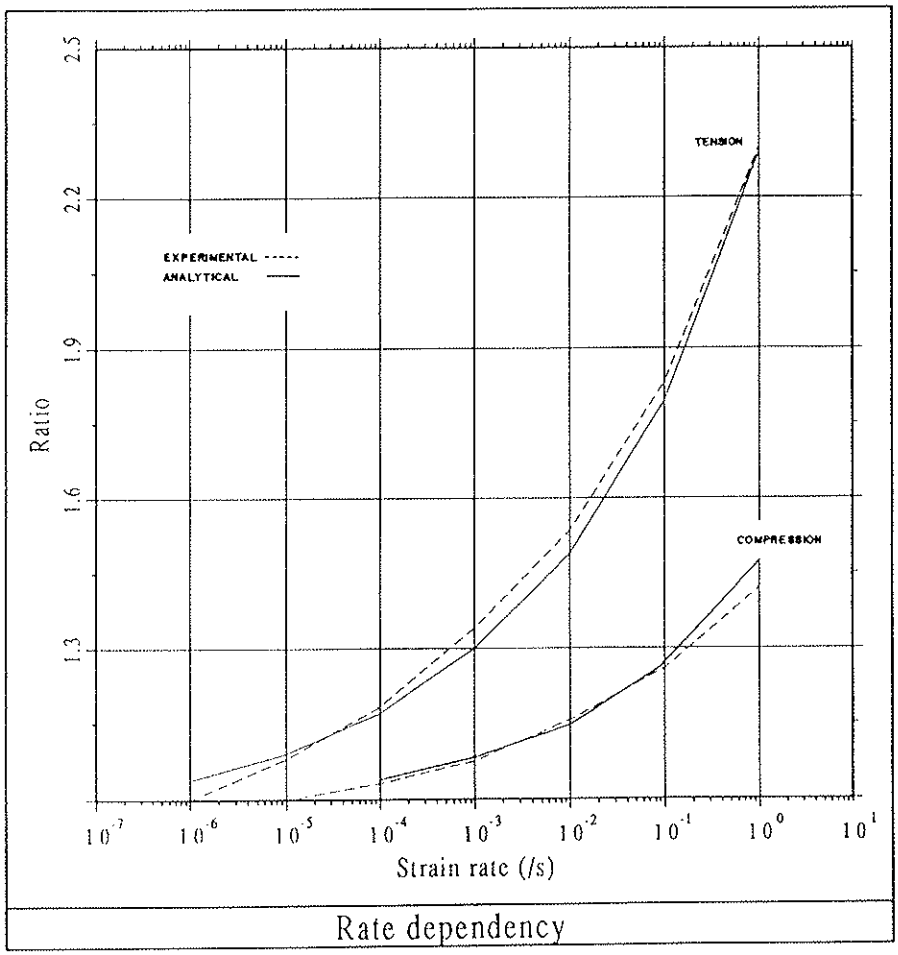

Figure 3.5 – Concrete rate dependency

Appendix A.1

DEFINITION OF THE EQUIVALENT STRESSES $\bar{\tau}^+$ AND $\bar{\tau}^-$

The definitions for tensile and compressive equivalent stresses $\bar{\tau}^+$ and $\bar{\tau}^-$ have been introduced on section 2.5, through equations (2.22) and (2.23). At that stage no further explanation was given for the particular (and in fact substantially different) forms postulated for these important entities. The reasons for such a procedure were that, by one hand it was not indispensable for the overall understanding of the material model which was about to be presented, and by other hand excessive detail would then be needed, introducing undesirable complexity.

A.1.1 – $\bar{\tau}^+$

For the equivalent stress $\bar{\tau}^+$ it was assumed the following scalar function of $\bar{\boldsymbol{\sigma}}^+$:

$$\bar{\tau}^+ = \sqrt{\bar{\boldsymbol{\sigma}}^+ : \mathbf{D}_0{}^{-1} : \bar{\boldsymbol{\sigma}}^+} \qquad (A.1.1)$$

From this definition it is clear that the 3D stress states having the same equivalent norm $\bar{\tau}^+$ define an ellipsoid centered on the origin of a space with axis $\bar{\sigma}_1$, $\bar{\sigma}_2$ and $\bar{\sigma}_3$ (the principal undamaged tensile stresses). If $\nu = 0$ the ellipsoid reduces to a sphere, and in the positive quadrant of the $\bar{\sigma}_1 - \bar{\sigma}_3$ effective stress space a quarter of a circle is obtained (see figure A.1.2), which can be considered a conservative envelope for the experimental results for concrete under tension-tension loading (see figure 1.2, form Kupfer *et al* experiments).

A.1.2 – $\bar{\tau}^-$

As it was pointed out in sections 2.11.3 and 2.11.4, under biaxial and triaxial compression concrete exhibits an enhanced strength, when compared

to the uniaxial peak strength. This feature cannot be captured by an equivalent stress like it was defined by equation (A.1.1), because $\bar{\tau}^-$ would increase as soon as some compressive confinement would be introduced together with a compressive axial stress, and so additional damage would be introduced for 2D and 3D compressive tests than for the uniaxial one.

To circunvent this situation, a different expression for $\bar{\tau}^-$ needs to be implemented. In this work the scalar function of $\bar{\boldsymbol{\sigma}}^-$

$$\bar{\tau}^- = \sqrt{\sqrt{3}\left(K\,\bar{\sigma}^-_{oct} + \bar{\tau}^-_{oct}\right)} \qquad (A.1.2)$$

was adopted, inspired on the Drucker-Pragger criterion.

As it is well known, the Drucker-Pragger criterion

$$\begin{aligned} F(\rho,\xi,\alpha,\kappa) &= \alpha\sqrt{6}\,\xi + \rho - \sqrt{2}\,\kappa = 0 \qquad (A.1.3)\\ \rho &= \sqrt{3}\,\tau_{oct}\\ \xi &= \sqrt{3}\,\sigma_{oct} \end{aligned}$$

defines a cone centered along hydrostatic axis, whose intersection with the octhaedral planes define circles with radius linearly increasing with the hydrostatic pressure. For this reason, tensile and compressive meridians are linear and symmetric respective to the hydrostatic axis (Oller (1988)), and so they can be represented on figure A.1.1 by a single straight line, which intersects axis $O\xi$ and $O\rho$ at coordinates $\kappa\,/\,(\alpha\sqrt{3})$ and $\sqrt{2}\,\kappa$.

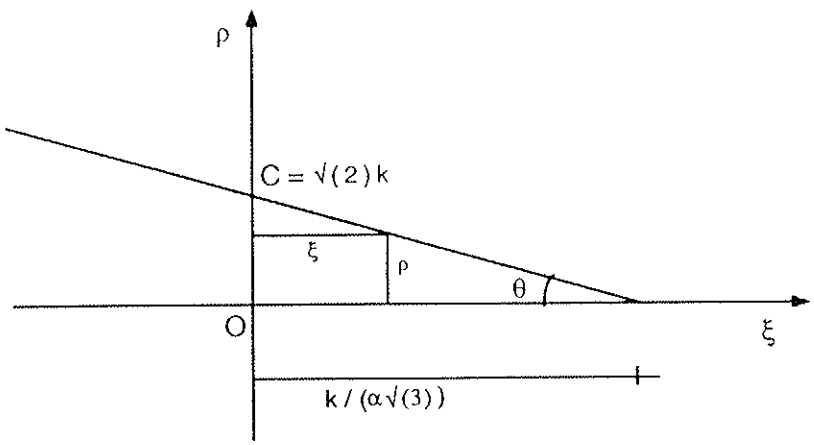

Figure A.1.1 – Drucker-Pragger criterion

Hence, it is geometrically evident that

$$\tan\theta = \frac{C-\rho}{\xi} = \frac{\sqrt{2}\,\kappa - \sqrt{3}\,\tau_{oct}}{\sqrt{3}\,\sigma_{oct}} \qquad (A.1.4)$$

which constitutes an alternative form for the Drucker-Pragger criterion.

The results from two distinct concrete compressive tests may then be considered for a proper evaluation of parameters $(\kappa,\ \theta)$. So, consider a 1D test $(\sigma_1 = 0,\ \sigma_2 = 0,\ \sigma_3)$ and a 2D one $(\sigma_1 = 0,\ \sigma_2 = \sigma_3)$, both driven so as to load concrete up to attaining threshold of nonlinearity. Denoting by $f_{0_{1D}}^{-}$ and $f_{0_{2D}}^{-}$ the maximum σ_3 elastic stresses obtained for the 1D and the 2D tests, it can be deduced that:

- Uniaxial test

$$\sigma_{oct_{1D}} = \frac{1}{3}\,tr\,(\boldsymbol{\sigma}) = \frac{1}{3}\,f_{0_{1D}}^{-} \qquad (A.1.5a)$$

$$\tau_{oct_{1D}} = \sqrt{\frac{2}{3}\,J_2} = -\frac{\sqrt{2}}{3}\,f_{0_{1D}}^{-} \qquad (A.1.5b)$$

- Biaxial test

$$\sigma_{oct_{2D}} = \frac{2}{3}\,f_{0_{2D}}^{-} \qquad (A.1.6a)$$

$$\tau_{oct_{2D}} = -\frac{\sqrt{2}}{3}\,f_{0_{2D}}^{-} \qquad (A.1.6b)$$

These compressive tests are associated to the same limit situation – the onset of nonlinearity – thus being represented by two distinct points on the initial Drucker-Pragger cone which separates the linear (elastic) and the nonlinear domains. According to expression (A.1.4) this conclusion can be expressed by

$$\tan\theta = \frac{\sqrt{2}\,\kappa - \sqrt{3}\,\tau_{oct_{1D}}}{\sqrt{3}\,\sigma_{oct_{1D}}} = \frac{\sqrt{2}\,\kappa - \sqrt{3}\,\tau_{oct_{2D}}}{\sqrt{3}\,\sigma_{oct_{2D}}} \qquad (A.1.7)$$

which is equivalent to

$$\left(\sqrt{2}\,\kappa - \sqrt{3}\,\tau_{oct_{1D}}\right)\sigma_{oct_{2D}} = \left(\sqrt{2}\,\kappa - \sqrt{3}\,\tau_{oct_{2D}}\right)\sigma_{oct_{1D}} \quad \Rightarrow$$

$$\Rightarrow \quad \kappa = \sqrt{\frac{3}{2}}\,\frac{\tau_{oct_{1D}}\,\sigma_{oct_{2D}} - \tau_{oct_{2D}}\,\sigma_{oct_{1D}}}{\sigma_{oct_{2D}} - \sigma_{oct_{1D}}} \qquad (A.1.8)$$

Substituting expressions (A.1.5) and (A.1.6) into (A.1.8), it is possible to express that

$$\kappa = \frac{1}{\sqrt{3}}\,\frac{f_{0_{1D}}^{-}\,f_{0_{2D}}^{-}}{f_{0_{1D}}^{-} - 2\,f_{0_{2D}}^{-}} \qquad (A.1.9)$$

So, constant

$$K = \tan\theta \tag{A.1.10}$$

can be evaluated substituting equation (A.1.9) into (A.1.7) and performing some mathematics:

$$\begin{aligned} K &= \frac{\sqrt{2}\,\kappa - \sqrt{3}\,\tau_{oct_{1D}}}{\sqrt{3}\,\sigma_{oct_{1D}}} = \frac{\sqrt{\frac{2}{3}}\left(\frac{f^-_{0_{1D}}\,f^-_{0_{2D}}}{f^-_{0_{1D}} - 2\,f^-_{0_{2D}}} + f^-_{0_{1D}}\right)}{\frac{1}{\sqrt{3}}\,f^-_{0_{1D}}} = \\ &= \sqrt{2}\,\frac{f^-_{0_{1D}}\,f^-_{0_{2D}} + f^-_{0_{1D}}\,f^-_{0_{1D}} - 2\,f^-_{0_{1D}}\,f^-_{0_{2D}}}{\left(f^-_{0_{1D}} - 2f^-_{0_{2D}}\right)f^-_{0_{1D}}} = \\ &= \sqrt{2}\,\frac{f^-_{0_{1D}} - f^-_{0_{2D}}}{f^-_{0_{1D}} - 2\,f^-_{0_{2D}}} \end{aligned} \tag{A.1.11}$$

Further simplification is introduced on this equation if the auxiliar variable

$$R_0 = \frac{f^-_{0_{2D}}}{f^-_{0_{1D}}} \tag{A.1.12}$$

is introduced, finally rendering for parameter K:

$$K = \sqrt{2}\,\frac{1 - R_0}{1 - 2\,R_0} \tag{A.1.13}$$

Now, the Drucker-Pragger criterion expressed through equation

$$C\left(\bar{\boldsymbol{\sigma}}\right) = \sqrt{3}\,\left(K\,\bar{\sigma}^-_{oct} + \bar{\tau}^-_{oct}\right) \tag{A.1.14}$$

provides the crucial idea from which the definition of the equivalent stress $\bar{\tau}^-$ has derived. In fact, variable C on (A.1.14) (see also figure A.1.1) can be regarded as a scalar norm of a 3D stress tensor, and so, if a square root of this norm is considered for the negative split of the effective stress tensor, it results:

$$\bar{\tau}^- = \sqrt{C\left(\bar{\boldsymbol{\sigma}}^-\right)} = \sqrt{\sqrt{3}\,\left(K\,\bar{\sigma}^-_{oct} + \bar{\tau}^-_{oct}\right)} \tag{A.1.15}$$

which coincides with expression (2.23).

A.1.3 – Damage bounding surface

According to the damage criteria introduced by equations (2.24) and (2.25), the bounding surface corresponding to the onset of damage is obtained when it is set

$$\bar{\tau}^{+} = \sqrt{\bar{\boldsymbol{\sigma}}^{+} : \mathbf{D_0}^{-1} : \bar{\boldsymbol{\sigma}}^{+}} = r_0^{+}$$
$$\bar{\tau}^{-} = \sqrt{\sqrt{3}\left(K\,\bar{\sigma}_{oct}^{-} + \bar{\tau}_{oct}^{-}\right)} = r_0^{-}$$

Depicting the possible 2D effective stress tensors which satisfy these conditions, a damage bounding surface similar to the one in figure A.1.2 is obtained

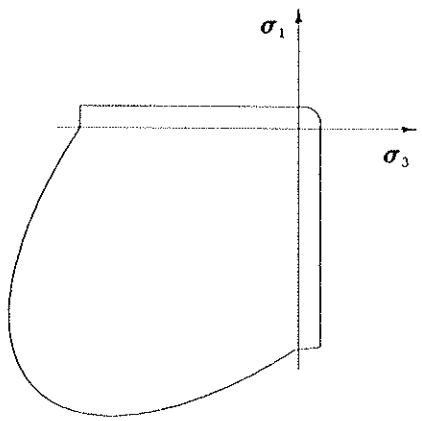

Figure A.1.2 – Initial damage bounding surface

Appendix A.2

DEFINITION OF PARAMETERS FOR PLASTIC-DAMAGE MODEL

A.2.1 – Tensile damage parameters r_0^+ and A^+

As it was referred on section 2.9.1 about the evolution of tensile damage variable

$$d^+ = G^+(\bar{\tau}^+) = 1 - \frac{r_0^+}{\bar{\tau}^+} e^{A^+\left(1-\frac{\bar{\tau}^+}{r_0^+}\right)} \qquad (A.2.1)$$

parameters r_0^+ and A^+ have to be specified. The former is very easy to determine: if f_0^+ is the 1D tensile strength beyond which nonlinear behavior initiates (see figure A.2.1), definition (2.22) allows to express that

$$r_0^+ = \sqrt{f_0^+ \frac{1}{E} f_0^+} = \frac{f_0^+}{\sqrt{E}} \qquad (A.2.2)$$

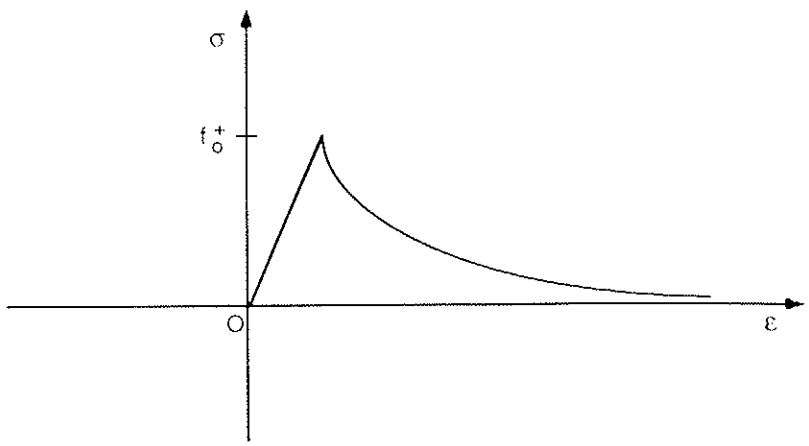

Figure A.2.1 – Stress-strain curve for 1D tensile test

Evaluation of A^+ is possible by introducing the concept of the specific dissipated energy on a 1D tensile process (Oliver *et al* (1990)):

$$g^+ = \int_0^\infty \dot{\gamma}\, dt \tag{A.2.3}$$

According to expression (2.65), on a pure tensile test the rate of dissipation is computed through

$$\dot{\gamma} = \Psi_0^+ \dot{d}^+ \tag{A.2.4}$$

As it also occurs that

$$\bar{\boldsymbol{\sigma}}^+ = \bar{\boldsymbol{\sigma}}$$

it is possible to express that

$$\Psi_0^+ = \frac{1}{2}\, \bar{\boldsymbol{\sigma}}^+ : \mathbf{D}_0^{-1} : \bar{\boldsymbol{\sigma}}^+ = \frac{(\bar{\tau}^+)^2}{2} \tag{A.2.5}$$

Introducing this conclusion into equation (A.2.4) and also keeping in mind the rate equation (2.31), it results that

$$\dot{\gamma} = \frac{(\bar{\tau}^+)^2}{2} \frac{dG^+}{d\bar{\tau}^+} \frac{d\bar{\tau}^+}{dt} \tag{A.2.6}$$

and so equation (A.2.3) can be expressed according to

$$g^+ = \frac{1}{2} \int_0^\infty (\bar{\tau}^+)^2 \frac{dG^+}{d\bar{\tau}^+} \frac{d\bar{\tau}^+}{dt}\, dt \tag{A.2.7}$$

or alternatively

$$g^+ = \frac{1}{2} \int_{r_0^+}^\infty (\bar{\tau}^+)^2 \frac{dG^+}{d\bar{\tau}^+}\, d\bar{\tau}^+ \tag{A.2.8}$$

Due to the definition considered on (A.2.1) for G^+, it is evident that

$$\begin{aligned} \frac{dG^+}{d\bar{\tau}^+} &= \frac{r_0^+}{(\bar{\tau}^+)^2}\, e^{A^+ (1-\frac{\bar{\tau}^+}{r_0^+})} + \frac{A^+}{\bar{\tau}^+} e^{A^+ (1-\frac{\bar{\tau}^+}{r_0^+})} = \\ &= e^{A^+} e^{-A^+ \frac{\bar{\tau}^+}{r_0^+}} \left(\frac{r_0^+}{(\bar{\tau}^+)^2} + \frac{A^+}{\bar{\tau}^+} \right) \end{aligned} \tag{A.2.9}$$

and so, applying standard integration rules,

$$g^+ = \frac{r_0^+}{2}\, e^{A^+} \left(\frac{-r_0^+}{A^+} \right) \left[e^{-A^+ \frac{\bar{\tau}^+}{r_0^+}} \right]_{r_0^+}^\infty +$$

$$+ \frac{A^+}{2} e^{A^+} \left(- \frac{r_0^+}{A^+} \left[\bar{\tau}^+ e^{-A^+ \frac{\bar{\tau}^+}{r_0^+}} \right]_{r_0^+}^{\infty} - \left(\frac{r_0^+}{A^+} \right)^2 \left[e^{-A^+ \frac{\bar{\tau}^+}{r_0^+}} \right]_{r_0^+}^{\infty} \right) =$$

$$= \frac{(r_0^+)^2}{2\,A^+} + \frac{(r_0^+)^2}{2} + \frac{(r_0^+)^2}{2\,A^+} =$$

$$= \left(\frac{1}{A^+} + \frac{1}{2} \right) (r_0^+)^2 \qquad (A.2.10)$$

Denoting by G_f the concrete fracture energy, and by l^* the charateristic length for the finite element which is being considered (Bažant *et al* (1979a), Bažant *et al* (1983)), elemental thermodynamics leads to the conclusion that

$$G_f = g^+ l^* \qquad (A.2.11)$$

and consequently parameter A^+ is obtained through the equation

$$A^+ = \left(\frac{G_f E}{l^* (f_0^+)^2} - \frac{1}{2} \right)^{-1} \qquad (A.2.12)$$

A.2.2 – Compressive damage parameters r_0^-, A^- and B^-

With reference to the compressive damage evolution law

$$d^- = 1 - \frac{r_0^-}{\bar{\tau}^-} (1 - A^-) - A^- e^{B^- (1 - \frac{\bar{\tau}^-}{r_0^-})} \qquad (A.2.13)$$

parameters A^- and B^- need to be specified, as well as threshold r_0^-.

Denoting by $f_{0_{1D}}^-$ the uniaxial stress for onset of nonlinear behavior and taking into consideration expressions (A.1.5) and (A.1.15), it is possible to write:

$$r_0^- = \sqrt{\frac{\sqrt{3}}{3} \left(K - \sqrt{2} \right) f_{0_{1D}}^-} \qquad (A.2.14)$$

and so, due to definition (A.1.13) for K, it is possible to calculate r_0^- according to:

$$r_0^- = \sqrt{\sqrt{\frac{2}{3}} \frac{R_0}{1 - 2\,R_0} f_{0_{1D}}^-} \qquad (A.2.15)$$

Evaluation of parameters A^- and B^- can be performed by imposing that the constitutive law satisfy two selected points of a 1D compressive test, thus rendering

$$\sigma = (1-d^-)\,\bar{\sigma} = \left(\frac{r_0^-}{\bar{\tau}^-}\,(1-A^-) + A^- e^{B^-\left(1-\frac{\bar{\tau}^-}{r_0^-}\right)}\right)\bar{\sigma} \qquad (A.2.16)$$

Considering that these points can be characterized by the *a priori* known entities[‡]:

- Point 1

  Cauchy stress σ_1

  Effective stress $\bar{\sigma}_1(\varepsilon_1) \;\Rightarrow$ Equivalent stress $\bar{\tau}_1^-$

- Point 2

  Cauchy stress σ_2

  Effective stress $\bar{\sigma}_2(\varepsilon_2) \;\Rightarrow$ Equivalent stress $\bar{\tau}_2^-$

it is then possible to state the following set of equations, which can be solved for evaluating parameters A^- and B^-:

$$\sigma_1 = \frac{r_0^-}{\bar{\tau}_1^-}\,\bar{\sigma}_1 + A^-\left(e^{B^-\left(1-\frac{\bar{\tau}_1^-}{r_0^-}\right)} - \frac{r_0^-}{\bar{\tau}_1^-}\right)\bar{\sigma}_1 \qquad (A.2.17a)$$

$$\sigma_2 = \frac{r_0^-}{\bar{\tau}_2^-}\,\bar{\sigma}_2 + A^-\left(e^{B^-\left(1-\frac{\bar{\tau}_2^-}{r_0^-}\right)} - \frac{r_0^-}{\bar{\tau}_2^-}\right)\bar{\sigma}_2 \qquad (A.2.17b)$$

Handling equation (A.2.17a), it results for A^-:

$$A^- = \frac{\sigma_1 - \frac{r_0^-}{\bar{\tau}_1^-}\,\bar{\sigma}_1}{\left(e^{B^-\left(1-\frac{\bar{\tau}_1^-}{r_0^-}\right)} - \frac{r_0^-}{\bar{\tau}_1^-}\right)\bar{\sigma}_1} \qquad (A.2.18)$$

[‡] The evaluation of $\bar{\sigma}_1$ and $\bar{\sigma}_2$ will be trivial after having determined the plastic parameter β, subject of section A.2.3.

which can be substituted into equation (A.2.17b), rendering

$$\sigma_2 - \frac{r_0^-}{\bar{\tau}_2^-}\bar{\sigma}_2 = \frac{\left(e^{B^-\left(1-\frac{\bar{\tau}_2^-}{r_0^-}\right)} - \frac{r_0^-}{\bar{\tau}_2^-}\right)\bar{\sigma}_2}{\left(e^{B^-\left(1-\frac{\bar{\tau}_1^-}{r_0^-}\right)} - \frac{r_0^-}{\bar{\tau}_1^-}\right)\bar{\sigma}_1}\left(\sigma_1 - \frac{r_0^-}{\bar{\tau}_1^-}\bar{\sigma}_1\right) \qquad (A.2.19)$$

Now, introducing the following definitions for a_1 and a_2 (which in fact are constants, because they only involve known entities)

$$a_1 = \left(\sigma_2 - \frac{r_0^-}{\bar{\tau}_2^-}\bar{\sigma}_2\right)\bar{\sigma}_1 \qquad (A.2.20a)$$

$$a_2 = \left(\sigma_1 - \frac{r_0^-}{\bar{\tau}_1^-}\bar{\sigma}_1\right)\bar{\sigma}_2 \qquad (A.2.20b)$$

equation (A.2.19) can assume the form

$$f\left(B^-\right) = a_1\left(e^{B^-\left(1-\frac{\bar{\tau}_1^-}{r_0^-}\right)} - \frac{r_0^-}{\bar{\tau}_1^-}\right) - a_2\left(e^{B^-\left(1-\frac{\bar{\tau}_2^-}{r_0^-}\right)} - \frac{r_0^-}{\bar{\tau}_2^-}\right) = 0 \qquad (A.2.21)$$

Solving of this nonlinear equation (with B^- being the unique unknown) can be performed by means of the iterative Newton-Raphson method (see expression (3.8)), according to the following recursive equation:

$$B_{i+1}^- = B_i^- - \frac{f\left(B_i^-\right)}{f'\left(B_i^-\right)} \qquad (A.2.22)$$

with $f'\left(B_i^-\right)$ given by:

$$f'\left(B_i^-\right) = a_1\left(1 - \frac{\bar{\tau}_1^-}{r_0^-}\right)e^{B^-\left(1-\frac{\bar{\tau}_1^-}{r_0^-}\right)} - a_2\left(1 - \frac{\bar{\tau}_2^-}{r_0^-}\right)e^{B^-\left(1-\frac{\bar{\tau}_2^-}{r_0^-}\right)} \qquad (A.2.23)$$

With such a procedure, combined with a convergence criterion, evaluation of parameter B^- is possible. Consequently, parameter A^- can also be trivially calculated, by substituting the already determined B^- into equation (A.2.18).

A.2.3 – Plastic parameter β

For evaluating parameter β, which accounts for plasticity, some reasoning on the basis of results from concrete experimental tests must be introduced.

Yankelevsky and Reinhardt (1987) compiled conclusions from many observed uniaxial cyclic compressive tests, introducing valuable guidelines to quantify plastic contribution on concrete behavior. Among several observations which they reported, it is possible to select the followings:

(i) The stress-strain envelope curves for a particular concrete submmited to several cyclic compressive tests are almost unique, furthermore coinciding with the one from a monotonic uniaxial experiment.

(ii) The unloading-reloading cycles can be reproduced by means of a graphical procedure, where use is made of six geometrical loci (termed *focal points*), which support the construction of the unloading-reloading cycles by means of picewise linear curves.

Concerning the attention to the most relevant feature within the context of the present section, that is, the plastic (or irreversible) strain upon unloading, figure A.2.2 schematizes a compressive envelope curve, as well the straight line $\overline{OE}$ and the focal points E, F, G, H, I, J. Excepting for J, the other focal points are located along line $\overline{OE}$, which is tangent to the envelope curve at the origin (hence, associated to the Young's modulus E).

Considering that points A and B are the starting and the ending points of a particular unloading cycle, it is evident that position of point B enables to quantify the amount of plastic deformation already experienced by concrete. It is also evident that point B can be determined by means of the intersection with the strain axis of the ray which connects point A and focal point F. Taking into consideration that coordinates for point A are $(\varepsilon_A, \sigma_A)$ and for point F (by imposition of the focal points model, in reference Yankelevsky and Reinhardt (1987)) are

$$\varepsilon_F = -\frac{f_u^-}{E}$$
$$\sigma_F = -f_u^-$$

it is then obvious that

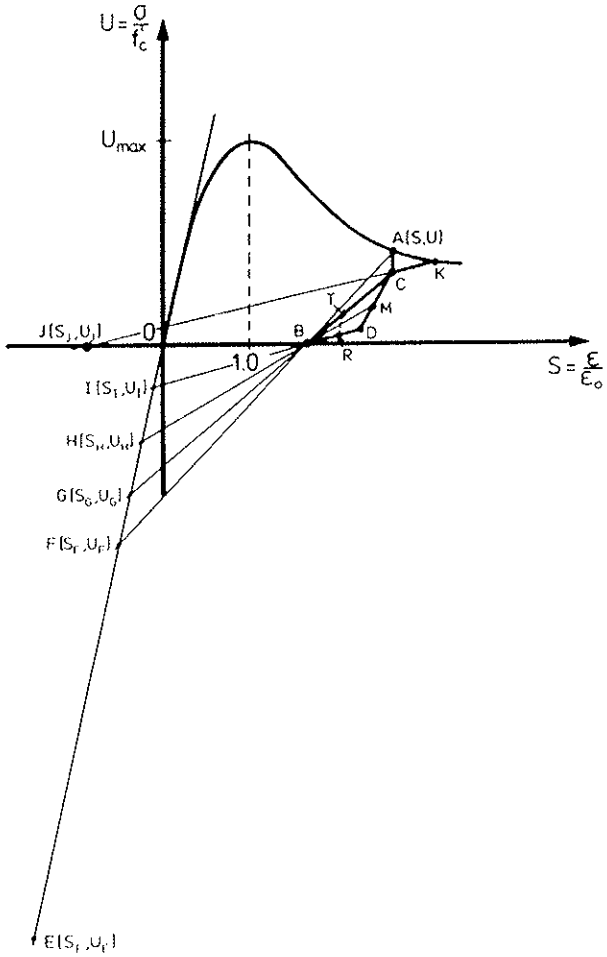

Figure A.2.2 – Focal points model (Yankelevsky and Reinhardt (1987))

$$\frac{0-\sigma_A}{\varepsilon_B-\varepsilon_A}=\frac{-f_u^-\;-\;0}{\frac{-f_u^-}{E}-\varepsilon_B}\quad\Rightarrow$$

$$\Rightarrow\quad \varepsilon_B=\frac{\varepsilon_A-\frac{\sigma_A}{E}}{\sigma_A+f_u^-}\,f_u^- \qquad (A.2.24)$$

Now, taking into consideration expression (2.5) and the hypothesis that during unloading no plastic evolution is supposed to take place, it results for

point B[‡]:

$$\bar{\sigma}_B = 0 = E(\varepsilon_B - \varepsilon_B^p) \qquad (A.2.25)$$

Furthermore, the postulated plastic strain evolution (equation (2.33)) enables to state (during compressive loading):

$$d\varepsilon^p = \beta\, d\varepsilon \qquad (A.2.26)$$

Integration of this equation allows to obtain the plastic strain which has been accumulated until the attainment of a certain level of global strain ε:

$$\varepsilon^p = \int_{\varepsilon_0}^{\varepsilon} \beta\, d\varepsilon = \beta(\varepsilon - \varepsilon_0) \qquad (A.2.27)$$

with

$$\varepsilon_0 = \frac{f_0^-}{E} \qquad (A.2.28)$$

being the strain associated to the uniaxial compressive stress where onset of damage and plasticity occurs, that is f_0^-.

Since during unloading (curve $\overline{AB}$) no evolution for plasticity occurs, it is possible to write that

$$\varepsilon_B^p = \varepsilon_A^p = \beta\left(\varepsilon_A - \frac{f_0^-}{E}\right) \qquad (A.2.29)$$

hence allowing to obtain (in accordance with equations (A.2.24) and (A.2.25)):

$$E\,\frac{\varepsilon_A - \frac{\sigma_A}{E}}{\sigma_A + f_u^-}\, f_u^- - \beta E\left(\varepsilon_A - \frac{f_0^-}{E}\right) = 0 \qquad (A.2.30)$$

So, selected a given point A $(\varepsilon_A, \sigma_A)$ for quantifying plastic effects, the evaluation of parameter β can be directly performed, according to

$$\beta = \frac{\left(\varepsilon_A - \frac{\sigma_A}{E}\right) f_u^-}{\left(\varepsilon_A - \frac{f_0^-}{E}\right)(\sigma_A + f_u^-)} \qquad (A.2.31)$$

---

‡ Notice that a 1D compressive test is being considered, hence with a unique non-null component.

Appendix A.3

INTRUCTIONS FOR ACCESSING THE PLASTIC-VISCOUS-DAMAGE CONSTITUTIVE MODEL IN OMEGA2

The described concrete material model has been implemented on program OMEGA2, and it can be selected by setting:

Model = 24

Besides the usual elastic constants

E – Young's modulus

NU – Poisson's coefficient

the following variables need also to be specified for accessing the proposed constitutive law, the meaning of each being evident from the notation which was adopted troughout the present text:

FTULT – 1D concrete tensile strength, which also coincides with the onset of nonlinearity, $f_u^+ = f_0^+$ (see section A.2.1)

GF – concrete tensile fracture energy, G_f (see section A.2.1)

FC01D – stress for onset of damage on 1D compressive tests, $f_{0_{1D}}^-$ (see section A.1.2)

RAT45 – ratio $R_0 = \frac{f_{0_{2D}}^-}{f_{0_{1D}}^-}$ (see section A.1.2)

STRA1 – strain for point 1 which defines 1D compressive stress-strain curve, ε_1 (see section A.2.2)

STRE1 – respective stress, σ_1 (see section A.2.2)

STRA2 – strain for point 2 which defines 1D compressive stress-strain curve, ε_2 (see section A.2.2)

STRE2 – respective stress, σ_2 (see section A.2.2)

FCU1D – 1D concrete compressive strength, f_u^- (see section A.2.3)

STRAP – strain for point A which controls plasticity, ε_A (see section A.2.3)

STREP – respective stress, σ_A (see section A.2.3)

FTENS – fluidity parameter for the evolution law of tensile damage variable (rate-dependency), ϑ_*^+ (see sections 3.2 and 3.4). Setting a negative value for this variable recovers the rate-independent model.

FCOMP – fluidity parameter for the evolution law of compressive damage variable (rate-dependency), ϑ_*^- (see sections 3.2 and 3.4). Setting a negative value for this variable recovers the rate-independent model.

EXPVT – exponent for the evolution law of tensile damage variable (rate-dependency), a^+ (see sections 3.2 and 3.4)

EXPVC – exponent for the evolution law of compressive damage variable (rate-dependency), a^- (see sections 3.2 and 3.4)

REFERENCES

Bažant, Zdeněk P.; Cedolin, Luigi (1979a) – Blunt Crack Band Propagation in Finite Element Analysis – *J. of Eng. Mech. Division, ASCE*, Vol. 105, N. EM2, pp. 297-315

Bažant, Zdeněk P.; Kim, Sang-Sik (1979b) – Plastic-Fracturing Theory for Concrete – *J. of Eng. Mech. Division, ASCE*, Vol. 105, N. EM3, pp. 407-428

Bažant, Zdeněk P.; Oh, B. H. (1983) – Crack Band Theory for Fracture of Concrete – *Matériaux et Constructions*, Vol. 16, N. 93, pp. 155-177

Bićanić, N.; Zienkiewicz, O. C. (1983) – Constitutive Model for Concrete under Dynamic Loading – *Earth. Eng. and Struct. Dyn.*, Vol. 11, pp. 689-710

Burden, Richard L.; Faires, J. Douglas (1985) – Numerical Analysis (third edition) – *Prindle, Weber & Schmidt*, Boston, USA

CEB, Comité Euro-International du Béton (1991) – Behavior and Analysis of Reinforced Concrete Structures under Alternate Actions Inducing Inelastic Response – *Bulletin d'Information N. 210*, Vol. 1 (General Models)

Cervera, M.; Oliver, J.; Oller, S.; Galindo, M. (1990) – "Pathological Behaviour" of Large Concrete Dams Analised via Isotropic Damage Models – *Proc. 2nd Int. Conf. on Comp. Aided Analysis and Design of Conc. Struct.*, Zell am See, Austria, pp. 633-643

Cervera, M.; Oliver, J.; Galindo, M. (1991) – Simulación Numérica de Patologías en Presas de Hormigón – *Monografia CIMNE N.4, Centro Internacional de Métodos Numéricos en Ingenieria* (in Spanish)

Chaboche, J. L. (1988a) – Continuum Damage Mechanics: Part I - General Concepts – *J. of Appl. Mech., Trans. of the ASME*, Vol. 55, pp. 59-64

Chaboche, J. L. (1988b) – Continuum Damage Mechanics: Part II - Damage Growth, Crack Initiation, and Crack Growth – *J. of Appl. Mech., Trans. of the ASME*, Vol. 55, pp. 65-72

Chappuis, Philippe (1987) – Modélisation Non-Linéaire du Comportement du Béton sous des Sollicitations Dynamiques – *PhD Thesis* N. 155, ETH - Swiss Federal Institute of Technology, Zurich, Switzerland (in French)

Chen, W. F. (1982) – Plasticity in Reinforced Concrete – *MacGraw-Hill*, New-York, USA

Green, S. J.; Swanson, S. R. (1973) – Static Constitutive Relations for Concrete – *AFWL-TR-72-244*, U.S. Air Force Weapons Laboratory, Kirtland Air Force Base, N. M.

Hall, John F. (1988) – The Dynamic and Earthquake Behavior of Concrete Dams: Review of Experimental Behavior and Observational Evidence – *Soil Dyn. and Earth. Eng.*, Vol. 7, N. 2

Ju, J. W. (1990) – Isotropic and Anisotropic Damage Variables in Continuum Damage Mechanics – *J. of Eng. Mech., ASCE*, Vol. 116, N. 12, pp. 2764-2770

Kachanov, L. M. (1958) – Time of Rupture Process Under Creep Conditions – *Izvestia Akademii Nauk, Otd Tech Nauk*, Vol. 8, pp. 26-31 (in Russian)

Kachanov, L. M. (1986) – Introduction to Continuum Damage Mechanics – *Martinus Nijhoff Publishers*

Krajcinovic, D.; Fonseka, G. U. (1981) – The Continuous Damage Theory of Brittle Materials - Part 1: General Theory – *J. of Appl. Mech., Trans. of the ASME*, Vol. 48, pp. 809-815

Kupfer, H.; Hilsdorf, H. K.; Rusch, H. (1969) – Behavior of Concrete under Biaxial Stresses – *J. Am. Concr. Inst.*, Vol. 66, N. 8, pp. 656-666

La Borderie, C.; Berthaud, Y.; Pijaudier-Cabot, G. (1990) – Crack Closure Effects in Continuum Damage Mechanics - Numerical Implementation – *Proc. 2nd Int. Conf. on Comp. Aided Analysis and Design of Conc. Struct.*, Zell am See, Austria, pp. 975-986

Lemaite, Jean; Chaboche, J. L. (1978) – Aspects Phénoménologiques de la Rupture par Endommagement – *J. Méc. Appl.*, Vol. 2, N. 3, pp. 317-365

Lemaitre, Jean (1984) – How to Use Damage Mechanics – *Nuclear Eng. and Design*, Vol. 80, pp. 233-245

Lemaitre, Jean (1985a) – Coupled Elasto-Plasticity and Damage Constitutive Equations – *Computer Meth. in Appl. Mech. and Eng.*, Vol. 51, pp. 31-49

Lemaitre, Jean (1985b) – A Continuous Damage Mechanics Model for Ductile Fracture – *J. of Eng. Mater. and Techn., Trans. of the ASME*, Vol. 107, pp. 83-89

Linsbauer, H. N.; Ingraffea, A. R.; Rossmanith, H. P.; Wawrzynek, P. A. (1989) – Simulation of Cracking in Large Arch Dam: Part I – *J. of Struct. Eng., ASCE*, Vol. 115, N. 7, pp. 1599-1615

Linsbauer, H. N.; Ingraffea, A. R.; Rossmanith, H. P.; Wawrzynek, P. A. (1989) – Simulation of Cracking in Large Arch Dam: Part II – *J. of Struct. Eng., ASCE*, Vol. 115, N. 7, pp. 1616-1630

Lubliner, J. (1972) – On the Thermodynamic Foundations of Non-Linear Solid Mechanics – *Int. J. Non-Linear Mech.*, Vol. 7, pp. 237-254

Lubliner, J.; Oliver J.; Oller S.; Oñate E. (1989) – A Plastic-Damage Model for Concrete – *Int. J. of Solids and Struct.*, Vol. 25, N. 3, pp. 299-326

Lubliner, Jacob (1990) – Plasticity Theory – *Macmillan Publishing Company*, NewYork, USA

Mazars, J.; Pijaudier-Cabot, G. (1989) – Continuum Damage Theory – Application to Concrete – *J. of Eng. Mech., ASCE*, Vol. 115, N.2, pp. 345-365

Mazars, J. (1991) – Damage Models for Concrete and their Usefulness for Seismic Loadings – *Experimental and Num. Meth. in Earth. Eng.*, J. Donea and P. M. Jones (eds.), pp. 199-221

Murakami, S. (1983) – Notion of Continuum Damage Mechanics and its Application to Anisotropic Creep Damage Theory – *J. of Eng. Mater. and Techn., Trans. of the ASME*, Vol. 105, pp. 99-105

Oliver, J.; Cervera, M.; Oller, S.; Lubliner, J. (1990) – Isotropic Damage Models and Smeared Crack Analysis of Concrete – *Proc. 2nd Int. Conf. on Comp. Aided Analysis and Design of Conc. Struct.*, Zell am See, Austria, pp. 945-957

Oller, Sergio (1988) – Un Modelo de "Daño Contínuo" para Materials Friccionales – PhD Thesis, E.T.S. Ingenieros de Caminos, Canales y Puertos, Technical University of Catalonia, Barcelona, Spain (in Spanish)

Oñate, E.; Oller, S.; Oliver, J.; Lubliner J. (1987) – A Constitutive Model for Cracking of Concrete Based on the Incremental Theory of Plasticity – *Computational Plasticity - Models, Software and Applications, Proc. of the International Conference held in Barcelona*, Spain, D. R. J. Owen, E. Hinton, E. Oñate (eds.)

Owen, D. R. J.; Hinton, E. (1980) – Finite Elements in Plasticity - Theory and Practice – *Pineridge Press Limited*, Swansea, United Kingdom

Póvoas, Rui F. (1991) – Modelos Não-Lineares de Análise e Dimensionamento de Estruturas Laminares de Betão Incluindo Efeitos Diferidos – *PhD Thesis*, Fac. of Eng., University of Oporto, Portugal (in Portuguese)

RILEM - International Union of Testing and Research Laboratories for Materials and Structures (1988) – Fracture Mechanics of Concrete - From Theory to Applications - Parts A, B – *Third Draft of a Report over the State of Art prepared by RILEM Technical Committee 90 - FMA*

Simo, J. C.; Ju, J. W. (1987a) – Strain- and Stress-Based Continuum Damage Models - I. Formulation – *Int. J. Solids Structures*, Vol. 23, N. 7, pp. 821-840

Simo, J. C.; Ju, J. W. (1987b) – Strain- and Stress-Based Continuum Damage Models - II. Computational Aspects – *Int. J. Solids Structures*, Vol. 23, N. 7, pp. 841-869

Sinha, B. P.; Gerstle, K. H.; Tulin, L. G. (1964) – Stress-Strain Relations for Concrete under Cyclic Loading – *J. Am. Concr. Inst.*, Vol. 62, N. 2, pp. 195-210

Suaris, Wimal; Shah, Surendra P. (1984) – Rate-Sensitive Damage Theory for Brittle Solids – *J. of Eng. Mech., ASCE*, Vol. 110, N. 6, pp. 985-997

Suaris, Wimal; Shah, Surendra P. (1985) – Constitutive Model for Dynamic Loading of Concrete – *J. of Struct. Eng., ASCE*, Vol. 111, N. 3, pp. 563-576

Suaris, Wimal; Ouyang, Chengsheng; Fernando, Viraj M. (1990) – Damage Model for Cyclic Loading of Concrete – *J. of Eng. Mech., ASCE*, Vol. 116, N. 5, pp. 1020-1035

Yankelevsky, David Z.; Reinhardt, Hans W. (1987) – Model for Cyclic Compressive Behavior of Concrete – *J. of Struct. Eng., ASCE*, Vol. 113, N. 2, pp. 228-240

Yankelevsky, David Z.; Reinhardt, Hans W. (1989) – Uniaxial Behavior of Concrete in Cyclic Tension – *J. of Struct. Eng., ASCE*, Vol. 115, N. 1, pp. 166-182

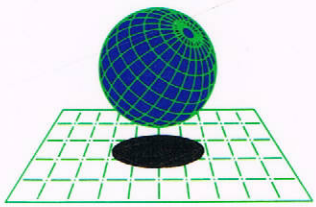

INTERNATIONAL
CENTER
FOR
NUMERICAL METHODS
IN ENGINEERING

Edificio C-1 Campus Norte-UPC, Gran Capitán, s/n. 08034 Barcelona-SPAIN · Phone 34-3-205 70 16 · Fax 34-3-401 65 17